cmgh
CELLULAR AND MOLECULAR GASTROENTEROLOGY AND HEPATOLOGY

ORIGINAL RESEARCH

Transcriptomic Dissection of Hepatocyte Heterogeneity: Linking Ploidy, Zonation, and Stem/Progenitor Cell Characteristics

Takeshi Katsuda,[1,*] Kazunori Hosaka,[1,2,*] Juntaro Matsuzaki,[1] Wataru Usuba,[1] Marta Prieto-Vila,[1,3] Tomoko Yamaguchi,[1,3] Atsunori Tsuchiya,[2] Shuji Terai,[2] and Takahiro Ochiya[1,3]

[1]*Division of Molecular and Cellular Medicine, National Cancer Center Research Institute, Chuo-ku, Tokyo, Japan;* [2]*Division of Gastroenterology and Hepatology, Graduate School of Medical and Dental Sciences, Niigata University, Aasahimachi-Dori, Chuo-Ku, Niigata, Japan;* [3]*Institute of Medical Science, Tokyo Medical University, Shinjuku, Tokyo, Japan*

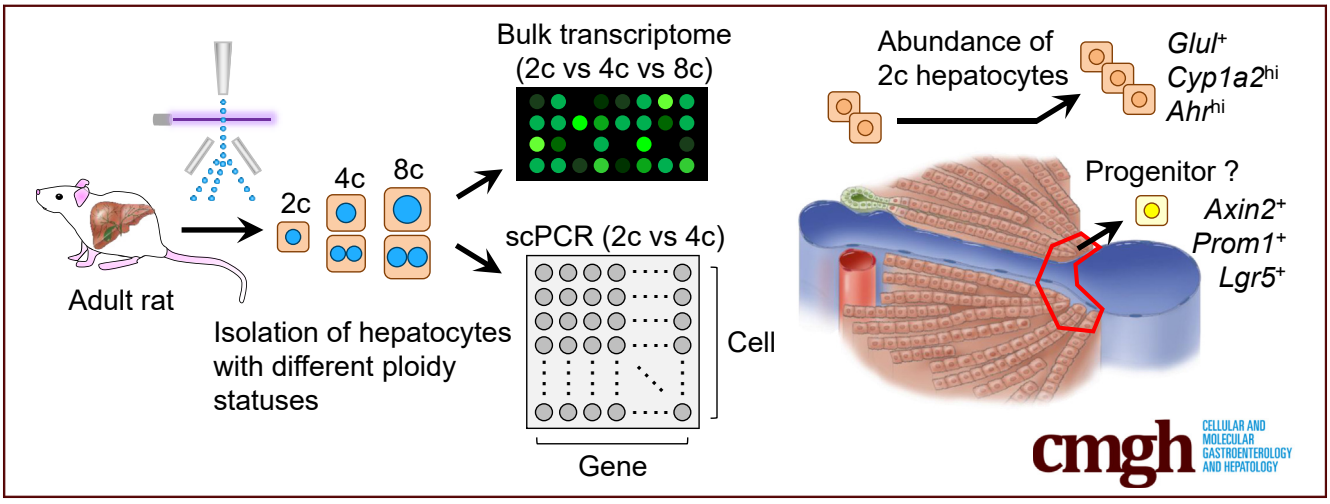

SUMMARY

By using rat hepatocytes with different ploidy statuses, a bulk transcriptome and single-cell quantitative reverse-transcription polymerase chain reaction show that diploid hepatocytes are preferentially located in the pericentral region. Single-cell analysis further identifies a subpopulation within the 2c hepatocytes that co-express the mature hepatocyte markers and liver progenitor cell markers.

BACKGROUND & AIMS: There is a long-standing debate regarding the biological significance of polyploidy in hepatocytes. Recent studies have provided increasing evidence that hepatocytes with different ploidy statuses behave differently in a context-dependent manner (eg, susceptibility to oncogenesis, regenerative ability after injury, and in vitro proliferative capacity). However, their overall transcriptomic differences in a physiological context is not known.

METHODS: By using microarray transcriptome analysis, we investigated the heterogeneity of hepatocyte populations with different ploidy statuses. Moreover, by using single-cell quantitative reverse-transcription polymerase chain reaction (scPCR) analysis, we investigated the intrapopulational transcriptome heterogeneity of 2c and 4c hepatocytes.

RESULTS: Microarray analysis showed that cell cycle–related genes were enriched in 8c hepatocytes, which is in line with the established notion that polyploidy is formed via cell division failure. Surprisingly, in contrast to the general consensus that 2c hepatocytes reside in the periportal region, in our bulk transcriptome and scPCR analyses, the 2c hepatocytes consistently showed pericentral hepatocyte-enriched characteristics. In addition, scPCR analysis identified a subpopulation within the 2c hepatocytes that co-express the liver progenitor cell markers *Axin2*, *Prom1*, and *Lgr5*, implying the potential biological relevance of this subpopulation.

CONCLUSIONS: This study provides new insights into hepatocyte heterogeneity, namely 2c hepatocytes are preferentially localized to the pericentral region, and a subpopulation of 2c hepatocytes show liver progenitor cell–like features in terms of liver progenitor cell marker expression (*Axin2*, *Prom1*, and *Lgr5*). *(Cell Mol Gastroenterol Hepatol 2020;9:161–183; https://doi.org/10.1016/j.jcmgh.2019.08.011)*

Keywords: Hepatocyte; Ploidy; Zonation; Single-Cell PCR; Transcriptome.

See editorial on page 193.

Polyploidy is a characteristic feature of hepatocytes, but its biological significance is largely unknown.[1–4] Hepatocytes are diploid (2c) at birth, but, after weaning,

their DNA content increases. In the adult rodent liver, up to 90% of hepatocytes are polyploid under physiological conditions.[5] The majority of polyploid hepatocytes are tetraploid (4c), but some are octoploid (8c) or even greater (≥16c). Although awareness of this heterogeneity is not new, whether hepatocytes with different ploidy statuses have different characteristics is still under debate.

Recent studies have provided evidence that hepatocytes with distinct ploidy statuses have different phenotypes. For example, Wang et al[6] showed that pericentral Axin2$^+$ hepatocytes are enriched with a 2c population and Axin2$^+$ 2c hepatocytes contribute to hepatocyte turnover and the maintenance of liver homeostasis. Our group found that 2c hepatocytes, in response to growth stimuli (ie, a small molecule cocktail), acquired a higher in vitro proliferative capacity than that of their 4c and 8c counterparts.[7] Similarly, Wilkinson et al[8] reported that the polyploid state restricts hepatocyte proliferation and liver regeneration. On the other hand, the hepatocyte polyploidization prevents tumorigenesis by decreasing their susceptibility to genomic aberrations.[8,9] These reports suggested that ploidy status affects the phenotype of hepatocytes; however, the studies have been focused on specific processes. More comprehensive analyses are required to gain broader, more holistic insights into this phenomenon.

In this study, we performed a microarray analysis to compare the transcriptomes of 2c, 4c, and 8c rat hepatocytes. In addition, to address any potential transcriptomic heterogeneity in hepatocytes with different ploidy statuses, we performed single-cell quantitative reverse-transcription polymerase chain reaction (scPCR) using a set of hepatocyte and liver progenitor cell (LPC) marker genes. Contrary to the widely accepted notion that 2c hepatocytes reside in the periportal region,[5,10–13] both our bulk transcriptome and scPCR results showed that 2c hepatocytes are preferentially located in the pericentral region. In addition, scPCR analysis showed the existence of a progenitor-like population of 2c hepatocytes.

Results

Microarray Transcriptome Analysis Identified 8c Hepatocytes as Cells With Typical Polyploid Characteristics

By using freshly isolated rat adult hepatocytes, we obtained 2c, 4c, and 8c hepatocytes using fluorescence-activated cell sorting (FACS) based on the fluorescence intensity of the DNA stain Hoechst 33342 (Figure 1*A*). We validated the accuracy of this sorting method by performing microscopic observations, which confirmed that none of the cells sorted into the 2c population were binucleated, whereas 42.0% ± 4.44% and 92.0% ± 7.10% of 4c- and 8c-sorted cells were binucleated, respectively (means ± SEM) (Figure 1*B* and *C*). Importantly, by phase-contrast imaging, we confirmed that the nucleus size of the mononucleated hepatocytes in the 4c fraction was larger than that in the 2c fraction (Figure 1*B*). Likewise, the nucleus size of the binucleated hepatocytes in the 8c fraction was larger than that in the 4c fraction (Figure 1*B*).

We next performed a microarray transcriptome analysis on the sorted populations of hepatocytes. After excluding probes without gene annotations and those with low expression levels (see the Materials and Methods section for details), we performed hierarchical clustering analysis at the whole-transcriptome level. As shown in Figure 2*A*, we did not observe a clear difference between 2c, 4c, and 8c hepatocytes. As expected, the expression levels of typical hepatocyte marker genes, including *Serpina1*, *Tf*, and *Ttr*, were almost the same in these 3 populations (Figure 2*B*), with an exception of the expression level of *Hnf4a* in 2c hepatocytes, which was slightly but significantly lower than the 8c counterpart.

Under physiological conditions, the polyploidization of hepatocytes is caused by cytokinesis failure during the cell cycle.[3,4] We found that most of the gene ontology (GO) bioprocess pathways enriched in 8c hepatocytes were associated with the cell cycle (Figure 2*C*). This observation was supported further by gene signature enrichment analysis (Figure 2*D*). Furthermore, we confirmed that the representative cell cycle– and cell division–associated genes were expressed at higher levels exclusively in 8c hepatocytes (Figure 2*E*). These results collectively show that the transcriptomes were overall similar among hepatocytes with different ploidy statuses, with the exception of the transcriptome of 8c hepatocytes. Thus, the transcriptome data are consistent with known differences between hepatocytes with different polyploidy statuses, indicating that the analysis was valid and biologically relevant.

2c Hepatocytes Show a Zone 3–Enriched Gene Signature

We reported previously that 2c hepatocytes and, to a lesser extent, 4c hepatocytes have in vitro colony forming ability in the presence of proliferative signals, whereas 8c hepatocytes do not[7] (reproduced in this study, as shown in Figure 3*A* and *B*). This finding emphasizes that, although the overall transcriptome is similar between 2c, 4c, and 8c hepatocytes, there must still be undetected differences among these populations. Indeed, unlike the hierarchical clustering analysis, in a principal component analysis (PCA), although the first principal component (PC1) did not separate the hepatocytes with different ploidy statuses, PC2 separated 2c hepatocytes from 4c and 8c hepatocytes (Figure 4*A*). As indicated by the plot labels in Figure 4*A*, PC1 reflects the variance derived from the batch difference of microarray

***Authors share co-first authorship.**

Abbreviations used in this paper: **ANOVA, analysis of variance; BEC, biliary epithelial cell; FACS, fluorescence-activated cell sorting; GO, gene ontology; LPC, liver progenitor cell; NPC, nonparenchymal cell; PCA, principal component analysis; RM, repeated-measures; scPCR, single-cell quantitative reverse-transcription polymerase chain reaction; TP, triple positive.**

Most current article

2352-345X
https://doi.org/10.1016/j.jcmgh.2019.08.011

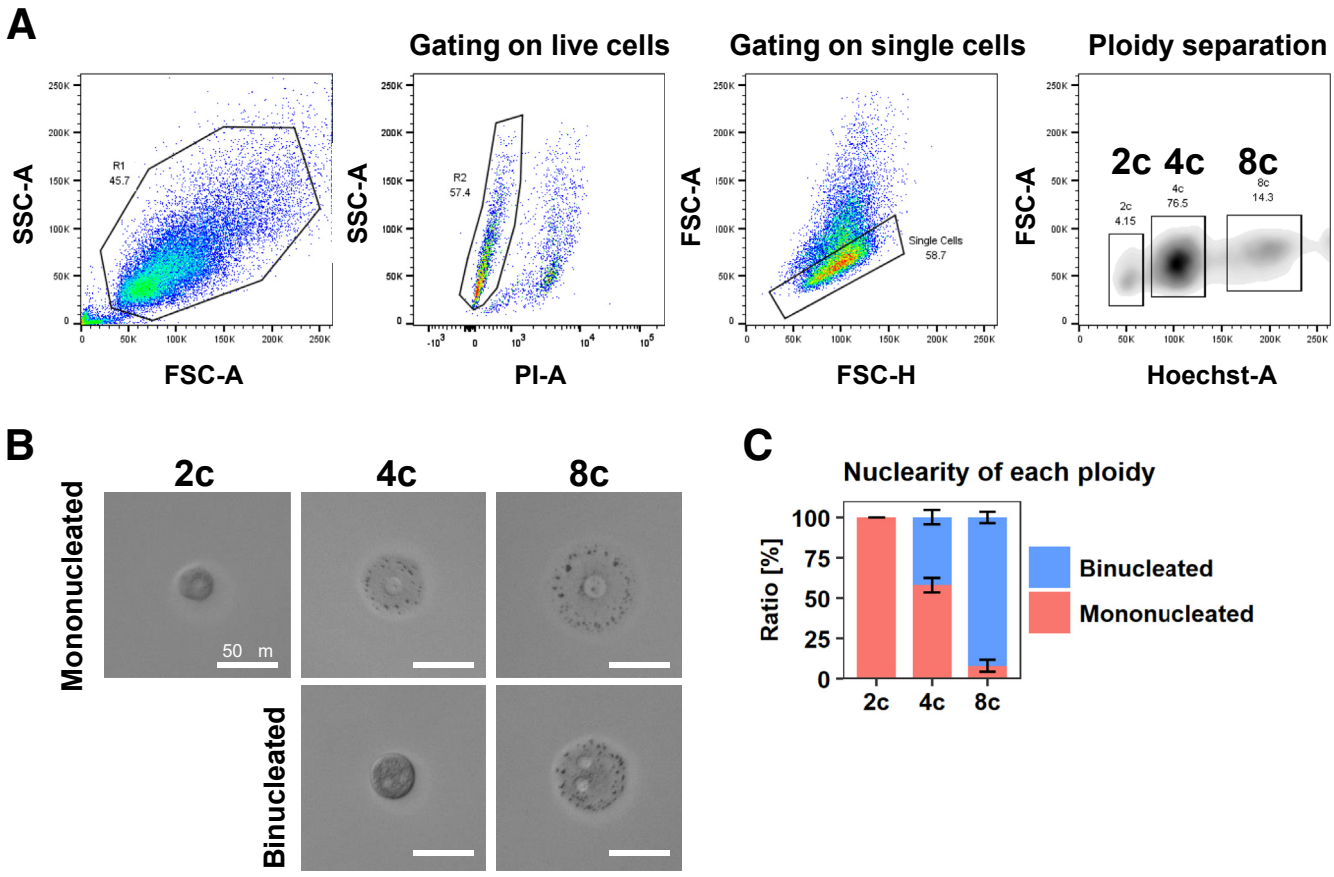

Figure 1. Validation of FACS sorting of hepatocytes with different ploidy statuses. (*A*) Representative gating for rat hepatocytes with 2c, 4c, and 8c DNA content as assessed by Hoechst 33342 fluorescent intensity. (*B*) Representative images of single-sorted 2c, 4c, and 8c hepatocytes. Ploidy statuses of the sorted hepatocytes were validated via microscopy on day 1 after plating. Images were taken using the BZX-710 microscope (Keyence). (*C*) Microscopic validation of nuclear numbers of hepatocytes. The data indicate the means ± SEM of 4 independent experiments. FSC-A, forward scatter-area; FSC-H, forward scatter-height; PI-A, propidium iodide-area; SSC-A, side scatter-area.

experiments. Given this technical issue, PC2-based information suggests that 2c hepatocytes have distinct phenotypes from 4c and 8c hepatocytes.

We further investigated for differentially expressed genes among these 3 populations. After filtering the probes with P values less than .05, determined by repeated-measures (RM) 1-way analysis of variance (ANOVA), we identified 3080 probes that were differentially expressed among 2c, 4c, and 8c hepatocytes. By using these probes, we performed hierarchical clustering, which confirmed that the 2c hepatocytes were distinct from the other 2 fractions (Figure 4*B*). A GO analysis identified multiple bioprocess pathways that were enriched in 2c hepatocytes. However, despite careful analysis, we could not identify meaningful patterns within these GO terms. We did not find any GO bioprocess pathways enriched in 4c hepatocytes, suggesting that these cells share most of the features of 2c and 8c hepatocytes.

We next asked whether ploidy status is associated with hepatic zone. The structure of the liver lobule generally is divided into 3 regions: zone 1 (periportal region), zone 3 (pericentral region), and zone 2 (intermediate region between zone 1 and zone 3). This hepatic zonation is the most well-characterized factor affecting the heterogeneity of hepatocytes in terms of phenotype, such as those related to metabolic and secretory functions.[14–17] We examined the expression of genes that have been reported to be enriched in zone 1, zone 2, and zone 3 hepatocytes.[18] We found that multiple zone 3–enriched genes were expressed at significantly higher levels in 2c hepatocytes (Figure 4*C*), including *Glul* ($P = 2.1 \times 10^{-5}$), *Cyp7a1* ($P = 3.4 \times 10^{-3}$), and *Slc1a2* ($P = 2.7 \times 10^{-5}$). We then manually prepared a "zone 3 signature gene set" by assembling 67 genes that were enriched significantly in zone 3 hepatocytes as reported by Halpern et al. Gene signature enrichment analysis showed that this zone 3 signature gene set was enriched significantly in 2c hepatocytes (nominal $P = .0082$) (Figure 4*D* and *E*). Consistently, 2c hepatocytes had higher Wnt signaling activity, a characteristic of the pericentral region (Figure 4*F*)[19,20]: nominal $P = .079$ for Wnt Signaling (contributed by SuperArray, Frederick, MA); nominal $P = .016$ for Kyoto Encyclopedia of Genes and Genomes (KEGG) _Wnt_signaling_pathway; $P = .055$ for WILLERT_Wnt_signaling (by the comparison of 2c vs 4c and 8c).

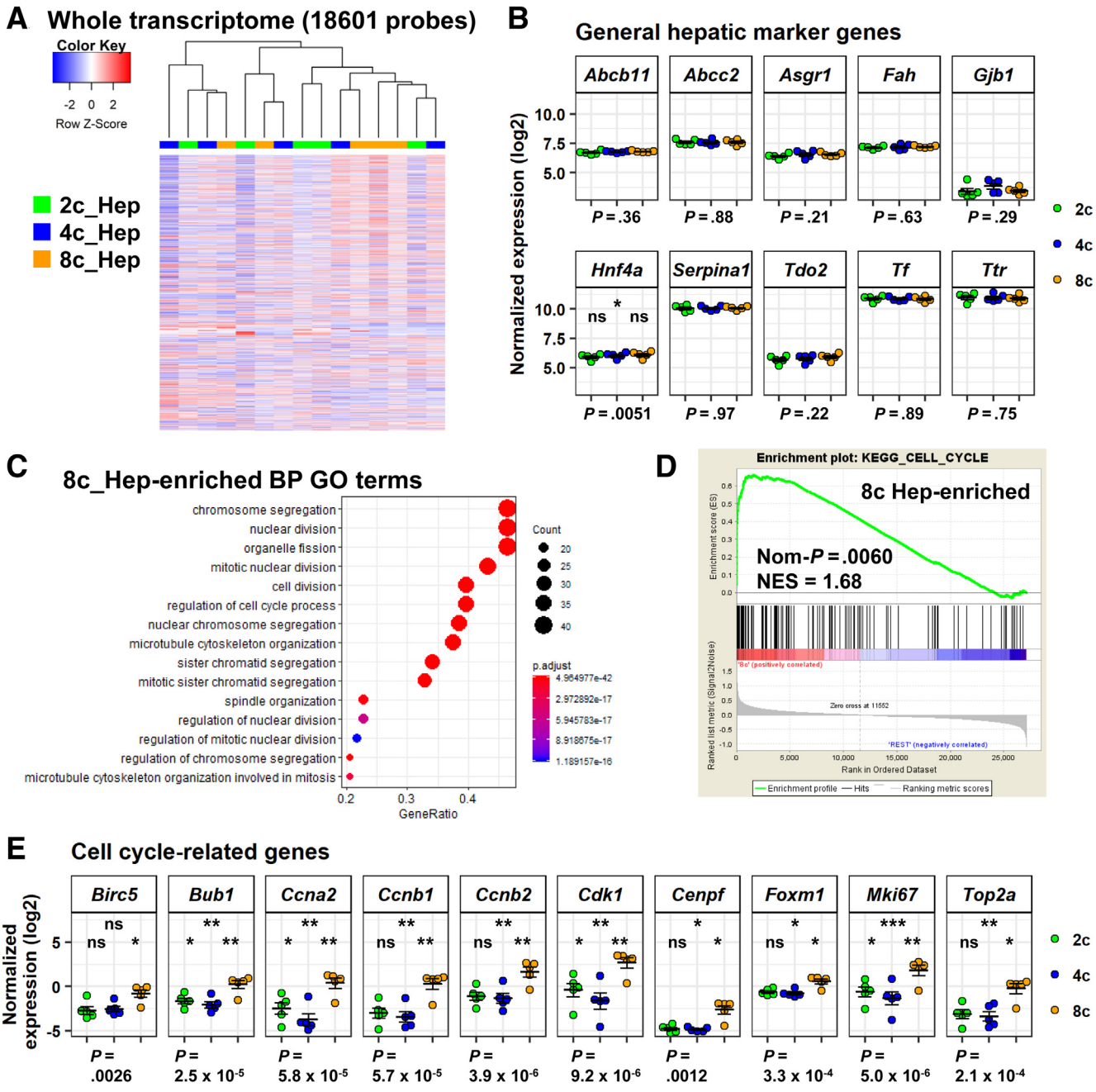

Figure 2. Microarray transcriptome analysis of rat hepatocytes with different ploidy statuses. (*A*) Heatmap with hierarchical clustering of whole-transcriptome analysis of 18,601 probes. Experiments were performed with 5 rats. (*B*) Expression of general hepatocyte marker genes. Data are means ± SEM (n = 5). (*C*) 8c hepatocyte-enriched pathways with GO terms (biological process) are shown. *Dots* represent term enrichment with color coding. The sizes of the *dots* represent the percentage of each GO term. (*D*) Gene signature enrichment analysis of 8c hepatocytes and 2c and 4c hepatocytes using the KEGG cell-cycle gene set. (*E*) Expression of cell cycle–related genes. Data are means ± SEM (n = 5). (*B* and *E*) Bottom: *P* values were calculated by RM 1-way ANOVA, followed by the Holm multiple comparisons test. *P* values for post hoc tests are presented as follows: $^{*}P < .05$, $^{**}P < .01$, $^{***}P < .001$. Significance symbols on the *left*, *middle*, and *right* in each panel indicate the comparison between 2c and 4c hepatocytes, 2c and 8c hepatocytes, and 4c and 8c hepatocytes, respectively. BP, biological process; KEGG, Kyoto Encyclopedia of Genes and Genomes; Nom, nominal.

Expression analysis of representative zone 1–enriched genes showed that several genes were significantly differentially expressed between the 3 fractions of hepatocytes, including *Asl* ($P = .0495$), *Ass1* ($P = .027$), and *G6pc* ($P = 1.1 \times 10^{-4}$) (Figure 5, top), but these differences were much smaller than those observed for zone 3–enriched genes (Figure 4*C*). As expected, nonmonotonic genes were expressed almost evenly throughout the 3 fractions

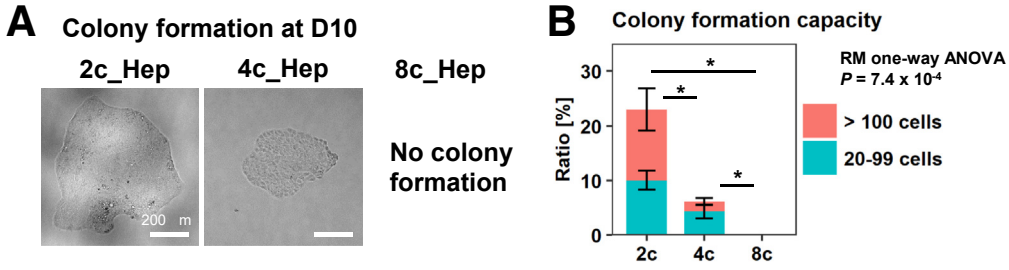

Figure 3. In vitro phenotypic validation of FACS-sorted hepatocytes. (*A*) Colony formation assay with single-sorted 2c, 4c, and 8c hepatocytes. Images were taken using the BZX-710 microscope (Keyence). (*B*) Colony-forming capacity was evaluated on day 10. Colonies with 20 or more cells were counted for each fraction. The data are shown as means ± SEM (n = 4). RM 1-way ANOVA was used to determine significant differences among the 3 groups ($P = 7.4 \times 10^{-4}$), followed by the Tukey–Kramer post hoc test as indicated in the panel. *$P < .05$. D, day.

(Figure 5, middle). By contrast, the expression levels of zone 2–enriched genes *Hamp* ($P = 2.1 \times 10^{-4}$) and *Igfbp2* ($P = 3.6 \times 10^{-4}$) were lower in 2c hepatocytes than in the other 2 fractions (Figure 5, middle). These results strongly suggest that 2c hepatocytes are enriched in zone 3.

Some LPC Marker Genes Are Expressed Differentially According to Ploidy Status

One question yet to be fully addressed is whether any specific subpopulation(s) of hepatocytes have stem/progenitor cell–like characteristics. Previous works have identified putative resident LPCs that are characterized by specific marker genes (eg, *Afp*, *Epcam*, and *Prom1/Cd133*) (reviewed by Miyajima et al[21]). Furthermore, several groups recently identified subsets of hepatocytes that phenotypically show LPC-like features,[6,22–24] while other groups have reported that mature hepatocytes have the capacity to be reprogrammed into LPCs.[25–30] In particular, Wang et al[6] recently reported that Axin2-positive pericentral hepatocytes, which contribute to hepatocyte turnover under physiological conditions, are enriched in 2c hepatocytes. Our analysis of zone 3–enriched genes showed that 2c hepatocytes showed a slightly but significantly higher expression of *Axin2* ($P = .024$) compared with the other hepatocyte populations (Figure 4*C*). In addition, other genes, including *Epcam* ($P = 9.7 \times 10^{-4}$), *Notch2* ($P = 2.5 \times 10^{-3}$), *Prom1* ($P = 1.0 \times 10^{-3}$), and *Tbx3* ($P = .012$), were expressed differentially with statistical significance (Figure 5, bottom).

Dissecting 2c and 4c Hepatocyte Heterogeneity at the Single-Cell Level

Microarray transcriptome analysis provided insight into the association between ploidy status and hepatic phenotype, but we were unable to determine whether the differences observed in the bulk analysis were attributable to global (averaged) differences between these fractions or to subpopulations that behave in a very different manner relative to the majority of the population. This question is particularly important when considering the existence of LPCs, which are supposed to be a rare population.

To examine the heterogeneity of hepatocytes from the point of view of different ploidy status, we performed scPCR analysis on FACS-sorted primary hepatocytes. To avoid contamination with doublet cells, we used the Fluidigm C1 system (Fluidigm, South San Francisco, CA), which is designed to capture cells with diameters ranging between 17 and 25 μm. Because the majority of 8c hepatocytes were larger than 25 μm (Figure 6*A*), the maximum diameter valid in the C1 platform, we excluded 8c hepatocytes from the scPCR analysis and focused on comparing 2c and 4c hepatocytes. We prepared a TaqMan probe set (Applied Biosystems, Beverly, MA) targeting 47 genes and 1 negative control (no probe added): these probes included 2 housekeeping genes, general hepatic marker genes, zone-related genes, biliary epithelial cell (BEC) marker genes, and LPC marker genes (Table 1). Because some of the LPC marker genes also are expressed by BECs, we first compared hepatocytes with the nonparenchymal cell (NPC) fraction, which contains BECs. We confirmed that 10 of 96 NPCs analyzed expressed *Krt19*, a definitive BEC marker, whereas only 2 of 337 hepatocytes, both of which were 2c, showed *Krt19* expression, which was lower than that in *Krt19*+ NPCs (Figure 6*B*). In particular, 5 of 10 *Krt19*+ NPCs expressed *Gstp1* and *Sox9*, which also are BEC markers, and thus we regarded these 5 NPCs as BECs. PCA of these 5 BECs and the 337 hepatocytes clearly discriminated the BECs from the hepatocytes (Figure 6*C*). Indeed, except for *Krt7*, which was not detected in our experiment and thus was excluded from the analysis, almost all of the BEC marker genes were expressed exclusively in BECs (Figure 6*B*). Accordingly, BECs showed no or much lower levels of expression of hepatocyte marker genes (Figure 6*B*). Importantly, the earlier-mentioned 2 *Krt19*-positive 2c hepatocytes were confirmed to be authentic hepatocytes because they showed robust expression of hepatic marker genes (eg, *Alb*, *Ttr*, and *G6pc*). A correlation heatmap for whole genes (43 genes, except *Krt7*, *Afp*, and *Ncam1*, which were expressed in <1% of analyzed cells) showed that the expression profiles of BEC/LPC markers and hepatocyte markers were clearly different (Figure 6*D*). Thus, we conclude that both the 2c and 4c hepatocytes investigated in this study were not contaminated with BECs.

By using 92 2c hepatocytes and 245 4c hepatocytes, we compared the expression levels of zone-related genes. A correlation heatmap of BEC/LPC makers (except *Krt19*,

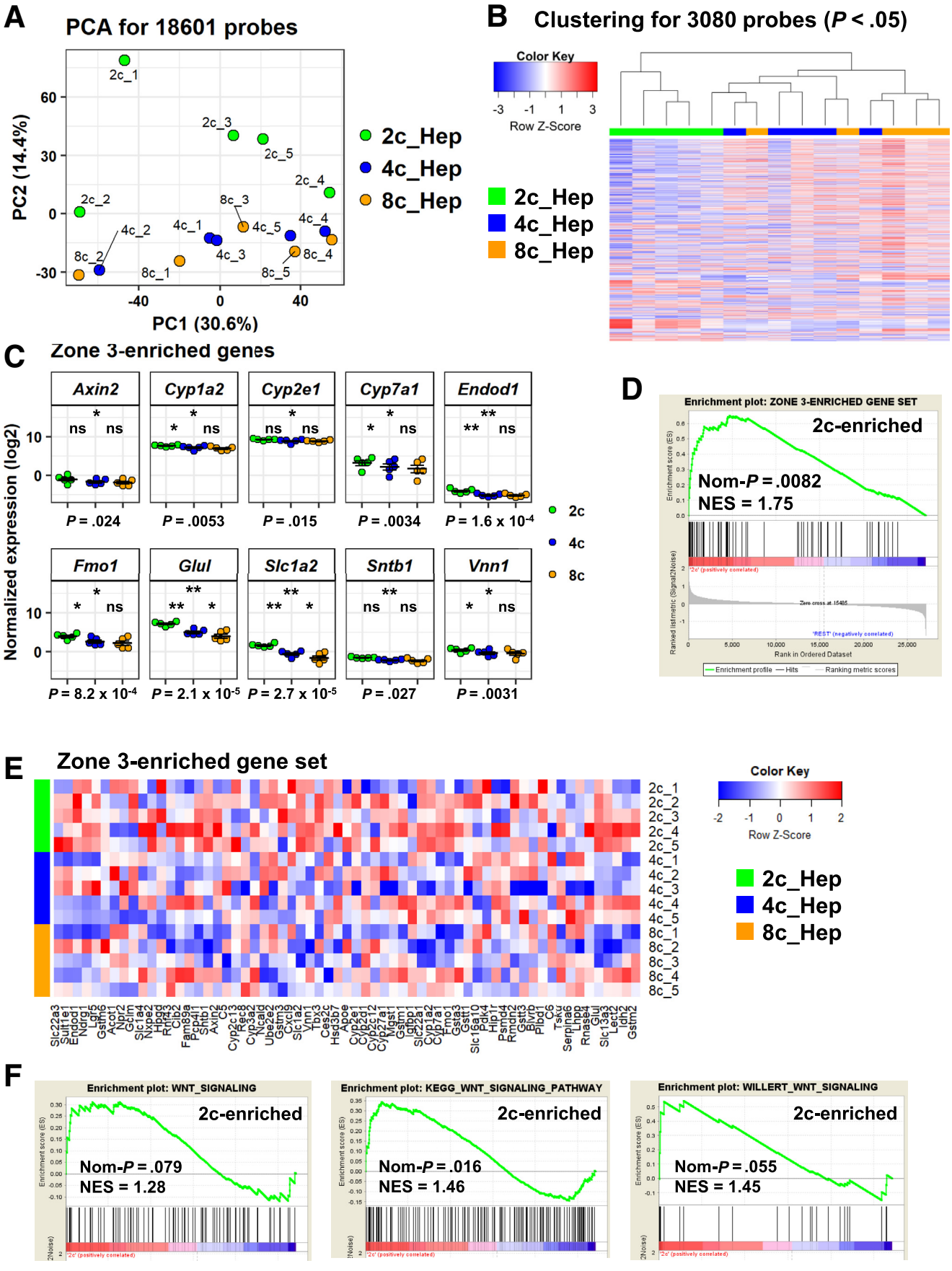
A
PCA for 18601 probes
PC2 (14.4%)
PC1 (30.6%)
2c_Hep
4c_Hep
8c_Hep
B
Clustering for 3080 probes (P < .05)
Color Key
Row Z-Score
C
Zone 3-enriched genes
Normalized expression (log2)
Axin2
Cyp1a2
Cyp2e1
Cyp7a1
Endod1
Fmo1
Glul
Slc1a2
Sntb1
Vnn1
D
Enrichment plot: ZONE 3-ENRICHED GENE SET
2c-enriched
Nom-P = .0082
NES = 1.75
E
Zone 3-enriched gene set
F
Enrichment plot: WNT_SIGNALING
Nom-P = .079
NES = 1.28
Enrichment plot: KEGG_WNT_SIGNALING_PATHWAY
Nom-P = .016
NES = 1.46
Enrichment plot: WILLERT_WNT_SIGNALING
Nom-P = .055
NES = 1.45

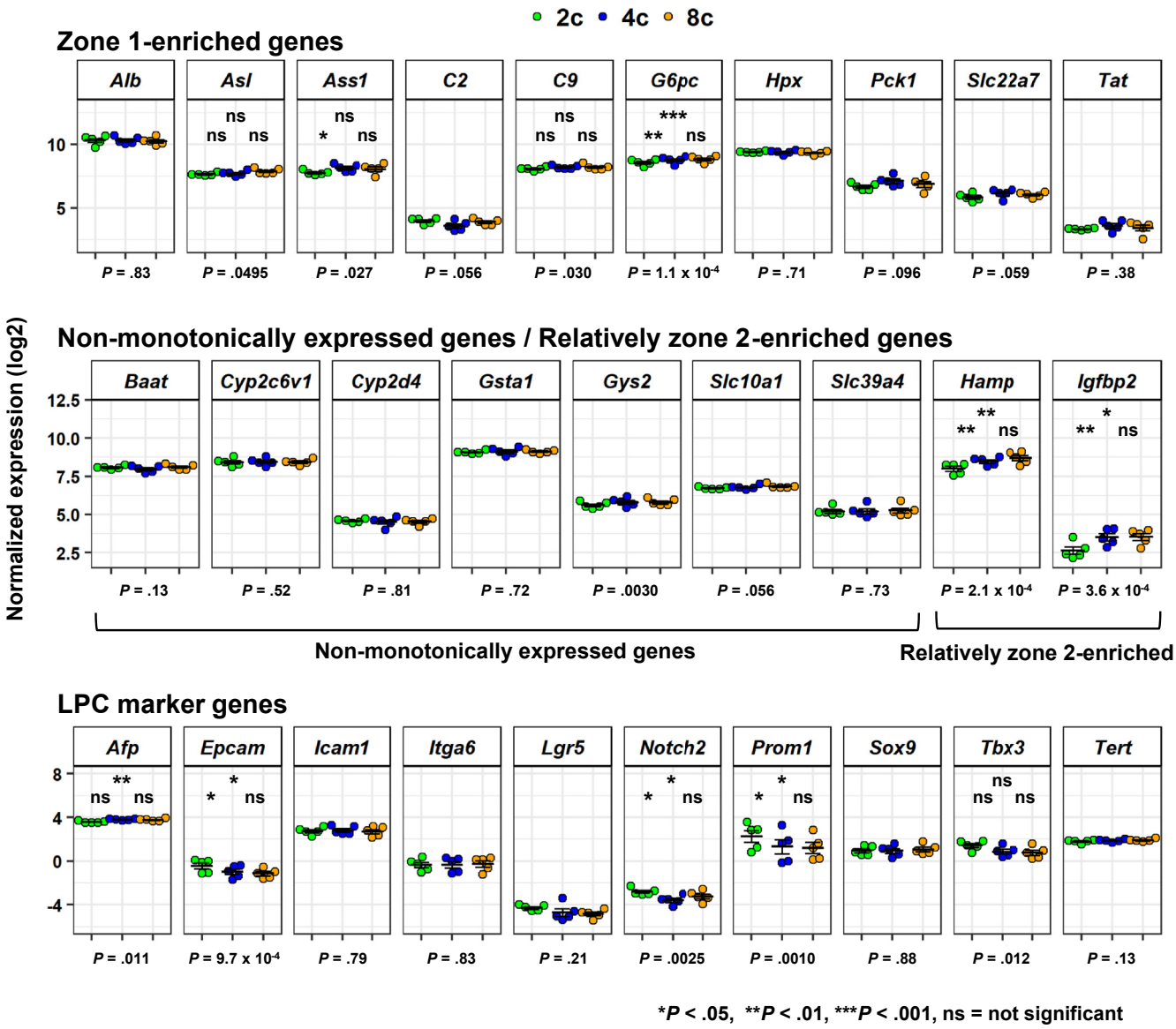

Figure 5. Further characterization of FACS-sorted hepatocytes. Expression of zone 1–enriched genes (*top*), non-monotonically expressed or relatively zone 2–enriched genes (*middle*), and LPC marker genes (*bottom*). Data are represented as means ± SEM (n = 5). *Bottom*: *P* values were calculated by RM 1-way ANOVA, followed by the Holm multiple comparisons test. *P* values for post hoc tests are presented as follows: $^{*}P < .05$, $^{**}P < .01$, $^{***}P < .001$. Significance symbols on the *left*, *middle*, and *right* in each panel indicate the comparison between 2c and 4c hepatocytes, 2c and 8c hepatocytes, and 4c and 8c hepatocytes, respectively.

Figure 4. (***See previous page***). **Characterization of differentially expressed genes in 2c, 4c, and 8c hepatocytes.** (*A*) PCA for whole-transcriptome analysis of 18,601 probes. Labels for each plot provide the ploidy information (2c, 4c, and 8c) with batch information of 5 experiments (_1, _2, _3, _4, and _5). (*B*) Heatmap with hierarchical clustering of the 3080 differentially expressed probes (defined as probes with $P < .05$ by RM 1-way ANOVA). (*C*) Expression of zone 3–enriched genes. Data are represented as means ± SEM (n = 5). *P* values at the bottom of each panel were calculated by RM 1-way ANOVA, followed by the Holm multiple comparisons test. *P* values for post hoc tests are presented as follows: $^{*}P < .05$, $^{**}P < 0.01$. Significance symbols on the *left*, *middle*, and *right* in each panel indicate the comparison between 2c and 4c hepatocytes, 2c and 8c hepatocytes, and 4c and 8c hepatocytes, respectively. (*D*) Gene signature enrichment analysis of 2c hepatocytes and 4c and 8c hepatocytes using a zone 3 signature gene set that was generated manually (the gene list is shown in panel *E*). (*E*) Heatmap of the zone 3–enriched gene set. (*F*) Gene signature enrichment analysis of 2c hepatocytes compared with 4c and 8c hepatocytes using Wnt signaling gene sets. KEGG, Kyoto Encyclopedia of Genes and Genomes; NES, Gene Set Enrichment Analysis; Nom, nominal.

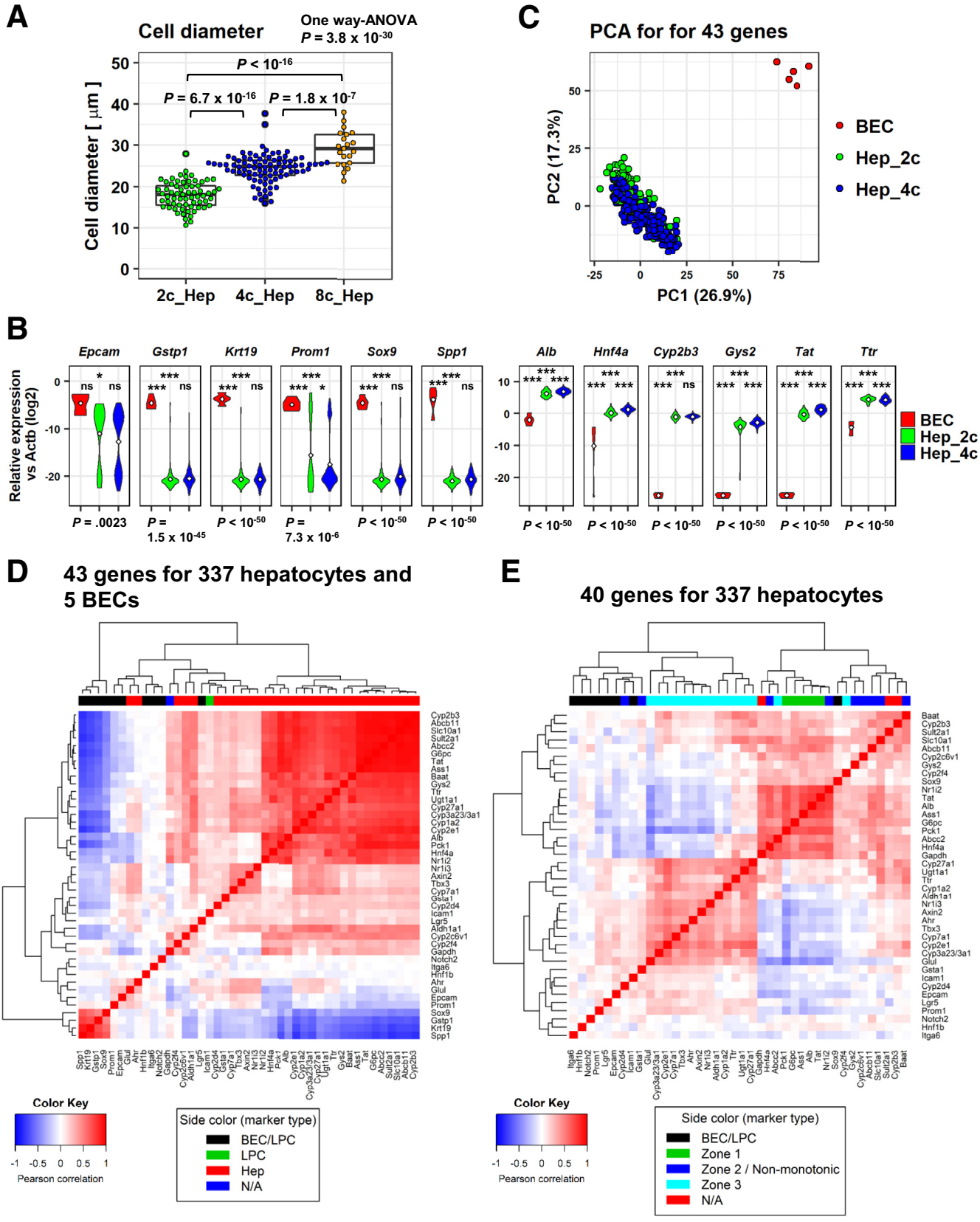
A
Cell diameter
One way-ANOVA
P = 3.8 x 10-30
P < 10-16
P = 6.7 x 10-16
P = 1.8 x 10-7
Cell diameter [μm]
2c_Hep
4c_Hep
8c_Hep
C
PCA for for 43 genes
PC2 (17.3%)
PC1 (26.9%)
BEC
Hep_2c
Hep_4c
B
Relative expression vs Actb (log2)
Epcam
Gstp1
Krt19
Prom1
Sox9
Spp1
Alb
Hnf4a
Cyp2b3
Gys2
Tat
Ttr
P = .0023
P = 1.5 x 10-45
P < 10-50
P = 7.3 x 10-6
D
43 genes for 337 hepatocytes and 5 BECs
Color Key
Pearson correlation
Side color (marker type)
BEC/LPC
LPC
Hep
N/A
E
40 genes for 337 hepatocytes
Side color (marker type)
BEC/LPC
Zone 1
Zone 2 / Non-monotonic
Zone 3
N/A

Gstp1, and *Spp1*, which were expressed in <1% of hepatocytes) and hepatic marker genes with zone information showed that hepatic genes were clustered in a zone-dependent manner (Figure 6*E*). Consistent with the observations from the bulk transcriptome, we confirmed that 2c hepatocytes showed higher expression levels for most of the zone 3–enriched genes (Figure 7*A*, middle).[18] Specifically, 94.6% of 2c hepatocytes expressed *Glul*, whose expression is sharply localized in proximity to the central vein, whereas only 58.8% of 4c cells expressed this gene. Accordingly, the zone 1–enriched genes *Alb* ($P = 4.2 \times 10^{-9}$), *Ass1* ($P = 3.2 \times 10^{-21}$), *G6pc* ($P = 1.6 \times 10^{-27}$), *Pck1* ($P = 1.3 \times 10^{-15}$), and *Tat* ($P = 2.5 \times 10^{-29}$) were expressed consistently at lower levels in 2c hepatocytes (Figure 7*A*, bottom left). We also confirmed that nonmonotonic genes were expressed at relatively similar levels in 2c and 4c hepatocytes (Figure 7*A*, bottom left). We also investigated the expression of LPC marker genes, including *Epcam*, *Icam1*, *Lgr5*, *Notch2*, *Prom1*, and *Tbx3*. Consistent with the bulk transcriptome results, *Epcam* ($P = .029$), *Prom1* ($P = .013$), *Tbx3* ($P = 1.0 \times 10^{-5}$), and *Axin2* ($P = 2.1 \times 10^{-6}$) were expressed at higher levels in 2c than in 4c hepatocytes (Figure 7*A*, bottom right, see middle for *Axin2*). In addition, we found that a small number of cells expressed *Lgr5*, whose expression levels were very low in the bulk microarray (Figure 5, bottom), presumably because the majority of hepatocytes, irrespective of their ploidy status, do not express this gene.[31] Hierarchical clustering of the 40 genes expressed in at least 1% of the total cells analyzed (≥4 cells) clustered the 2c and 4c hepatocytes into distinct groups (Figure 7*B*, lower column side bar). As highlighted in the upper column side bar (see the purple-colored cluster on the far left), the 2c hepatocyte-rich subpopulation showed higher expression of multiple LPC markers including *Axin2*, *Prom1*, and *Lgr5* (Figure 7*B*, upper column side bar).

PCA of Single Cells Using Zonation and LPC Signature

We next visualized each of the analyzed cells by PCA and confirmed that the 2c and 4c hepatocytes form distinct populations (Figure 8*A*). Loading these PCA plots with the expression levels of zone-associated genes indicated that 2c hepatocytes have a pericentral expression signature (Figure 8*B*–*D*). Some of the 4c hepatocytes expressed zone 3 marker genes, including *Axin2*, *Cyp7a1*, and *Nr1i3* (Figure 8*B*, dotted ellipses), showing that not only 2c but also 4c hepatocytes distribute to zone 3. However, the highest expression levels of *Glul*, *Cyp1a2*, and *Cyp2e1* were almost restricted to the 2c cells (Figure 8*B*, solid ellipses). Indeed, the top 10% of cells ranked according to *Glul* expression level (34 of 337 cells) were 2c hepatocytes. Convincingly, cells with the highest expression of *Glul* showed lower expression levels of zone 1–enriched genes such as *Alb*, *Ass1*, *G6pc*, *Pck1*, and *Tat* (Figure 8*C*, solid ellipses). On the other hand, the subpopulation of 4c hepatocytes with partial expression of zone 3 marker genes also exhibited high expression levels of zone 1–enriched genes (Figure 8*C*, dotted ellipses). Compared with zone 1– and zone 3–enriched genes, we confirmed that 2c-enriched/nonmonotonic genes showed similar levels of expression among the analyzed cells (Figure 8*D*).

As described earlier, hierarchical clustering showed a 2c hepatocyte-rich subpopulation that was enriched with cells expressing *Axin2*, *Prom1*, and *Lgr5* (Figure 7*B*). A Venn diagram of the whole hepatocyte population indicated that 100% (20 of 20) and 70.0% (14 of 20) of *Lgr5*+ hepatocytes expressed *Axin2* and *Prom1*, respectively, and that 82.9% (68 of 82) of *Prom1*-positive hepatocytes expressed *Axin2* (Figure 9*A*). These results were suggestive of a population hierarchy among LPC marker–expressing hepatocytes in which a population positive for all 3 LPC markers (hereafter designated as *triple positive* [TP] population) resided at the top. The TP population comprised 4.15% of the entire hepatocyte pool (14 of 337 hepatocytes). The abundancy of TP cells was higher in 2c hepatocytes (12.0%; 11 of 92 cells) than in 4c hepatocytes (1.2%; 3 of 245 cells) (Figure 9*B*, see also Figure 9*C* for detailed co-expression profiles), confirming that the TP population is highly enriched among 2c hepatocytes.

We further explored the expression profiles of all of the LPC markers, including *Lgr5*, *Axin2*, *Prom1*, *Epcam*, *Icam1*, *Sox9*, and *Notch2* in the TP population. We found that the TP population also was enriched for *Epcam*, *Icam1*, and *Tbx3* (Figure 9*B*). By contrast, these cells did not express *Sox9* (Figure 9*B*). *Sox9* expression is reported to be limited to a subpopulation of zone 1 hepatocytes called "hybrid hepatocytes."[23,32] Thus, the TP population can be regarded as a population distinct from hybrid hepatocytes. We also confirmed that all of the TP population cells (14 of 14) expressed *Glul*, strongly suggesting that these cells are localized to the pericentral region. Indeed, Planas-Paz et al[33] recently reported that, in mice, *Lgr5* messenger RNA expression was observed preferentially in pericentral hepatocytes.

Figure 6. (***See previous page***). **Validation of the results of scPCR.** (*A*) Cell size of FACS-sorted 2c, 4c, and 8c hepatocytes. A total of 65, 88, and 21 cells were analyzed for 2c, 4c, and 8c cells, respectively. One-way ANOVA was used to determine significant differences among the 3 groups ($P = 3.8 \times 10^{-30}$), followed by the Tukey multiple comparisons test. (*B*) Violin plots of BEC marker genes (*left*) and hepatocyte marker genes (*right*). Bottom: *P* values were calculated by 1-way ANOVA, followed by the Tukey multiple comparisons test. *P* values for post hoc tests are presented as follows: $^{*}P < .05$, $^{***}P < .001$. Significance symbols on the *left*, *middle*, and *right* in each panel indicate the comparison between BEC and 2c hepatocytes, BEC and 4c hepatocytes, and 2c and 4c hepatocytes, respectively. (*C*) PCA of 2c and 4c hepatocytes with 5 *Krt19*$^{+}$*Sox9*$^{+}$*Gstp1*$^{+}$ BECs using 43 genes. (*D*) Correlation heatmap for whole genes (43 genes, except *Krt7*, *Afp*, and *Ncam1*, which were expressed in <1% of the analyzed cells) using 5 BECs and 337 hepatocytes. (*E*) Correlation heatmap of BEC/LPC makers (except *Krt19*, *Gstp1*, and *Spp1*, which were expressed in <1% of hepatocytes) and hepatic marker genes with zone information.

Table 1. Gene List for scPCR Analysis

Gene	House keeping marker	Zone 1 marker	Zone 2/ nonmonotonic marker	Zone 3 marker	LPC marker	BEC marker	Description/note	Reference
Actb Rn00667869_m1	○						Reported to have no zonation[18] Used for normalizing gene expression	18
Gapdh Rn01775763_g1	○						Reported to have no zonation, but relatively more deviated than *Actb*[18]	18
Alb Rn00592480_m1		○					Hepatocyte-secreted serum protein	15,18
Tat Rn00562011_m1		○					Hepatocyte-secreted serum protein	18
Ass1 Rn00565808_g1		○					Involved in the synthesis of creatine, polyamines, arginine, urea, and nitric oxide	18
G6pc Rn00689876_m1		○					Functions in gluconeogenesis and glycogenolysis	18,53
Pck1 Rn01529014_m1		○					Main regulator in gluconeogenesis	15,18,54
Abcb11 Rn01515444_m1			○				ABC transporter expressed along bile canaliculi	18
Cyp2c6v1 Rn03417171_gH			○				Phase I modification enzyme	7
Cyp2d4 Rn01504629_m1			○				Phase I modification enzyme A rat orthologue of human *CYP2D6* and mouse *Cyp2d22*	18
Gsta1 Rn04223027_m1			○				Phase II conjugation enzyme	18
Baat Rn00568867_m1			○				Catalyzes the transfer of C24 bile acids from the acyl-CoA thioester to either glycine or taurine	18
Gys2 Rn00565296_m1			○				Catalyzes the rate-limiting step in the synthesis of glycogen	18
Slc10a1 Rn00566894_m1			○				Bile acid transporter located at the basal side of hepatocytes	18
Nr1i2 Rn00583887_m1			○				Detected in no more than 1% of analyzed cells, thus not included in analysis	18
Sult2a1 Rn04223057_mH			○				Phase II conjugation enzyme	Human protein atlas: www.proteinatlas.org
Glul Rn01483107_m1				○			Catalyzes the synthesis of glutamine from glutamate and ammonia	15,18,54–56
Sult2a1 Rn04223057_mH				○			ABC transporter expressed along bile canaliculi	18

Table 1. Continued

Gene	House keeping marker	Zone 1 marker	Zone 2/ nonmonotonic marker	Zone 3 marker	LPC marker	BEC marker	Description/note	Reference
Aldh1a1 Rn00755484_m1				○			The next enzyme after alcohol dehydrogenase in the alcohol metabolism pathway	18
Ahr Rn00565750_m1				○			Transcription factor that regulates Cytochrome P450 (CYP) enzyme expression	15,16,18,55,56
Nr1i3 Rn04339043_m1				○			Nuclear receptor, also known as constitutive androstane receptor, which regulates xenobiotic and endobiotic metabolism	15,18,56
Cyp1a2 Rn00561082_m1				○			Phase I modification enzyme	15,16,18,55,56
Cyp2e1 Rn00580624_m1				○			Phase I modification enzyme	15,16,18,54–56
Cyp2f4 Rn00570779_m1				○			Phase I modification enzyme A rat orthologue of mouse *Cyp2f2*	18,55
Cyp3a23 /3a1 Rn01412959_g1				○			Phase I modification enzyme	16
Cyp7a1 Rn00564065_m1				○			Phase I modification enzyme	7,18,55
Cyp27a1 Rn00710297_m1				○			Phase I modification enzyme	16,18,55
Hnf4a Rn04339144_m1				○			Transcription factor that plays an important role in liver development and liver functions	18
Ugt1a1 Rn00754947_m1				○			Phase II conjugation enzyme	16,18
Ttr Rn00562124_m1				○			Hepatocyte-secreted serum protein	18
Cyp2b3 Rn01476084_m1							Phase I modification enzyme No zonation-related information available	N/A
Axin2 Rn00577441_m1				○	○		Plays an important role in the regulation of the stability of β-catenin	6,15,18
Tbx3 Rn00710902_m1				○	○		Transcription factor involved in the regulation of various developmental processes	18
Sox9 Rn01751070_m1		○			○	○	Transcription factor regulating the bile duct development of BECs Also reported to be expressed by periportal adult LPCs	23,32,57
Afp Rn00560661_m1					○		A major plasma protein produced by fetal liver cells Also expressed by injury-induced rat LPCs	21
Ncam1 Rn01418541_m1					○	○	A marker expressed in developing bile ducts and LPCs	58,59

Table 1. Continued

Gene	House keeping marker	Zone 1 marker	Zone 2/ nonmonotonic marker	Zone 3 marker	LPC marker	BEC marker	Description/note	Reference
Epcam Rn01473202_m1					○	○	A marker expressed in fetal hepatoblasts, BECs, and injury-induced adult LPCs	[21]
Prom1 Rn00572720_m1					○	○	A marker expressed in fetal hepatoblasts, BECs, and injury-induced adult LPCs	[21]
Notch2 Rn01534371_m1					○		A marker expressed in fetal hepatoblasts	[60]
Icam1 Rn00564227_m1					○	○	A marker expressed in fetal hepatoblasts, BECs, and injury-induced adult LPCs	[61]
Itga6 Rn01512708_m1					○	○	A marker expressed in fetal hepatoblasts, BECs, and injury-induced adult LPCs	[21]
Lgr5 Rn01509662_m1					○	○	A marker expressed in BECs/LPCs upon injury	[31]
Krt19 Rn01496867_m1						○	A marker of BECs	[62]
Krt7 Rn04224249_u1						○	A marker of BECs Detected in <1% of analyzed cells, thus excluded from study	[62]
Gstp1 Rn00561378_gH					○	○	A marker of BECs and LPCs	[63–65] Human protein atlas: www.proteinatlas.org
Hnf1b Rn00447453_m1						○	A marker of BECs	[62]
Spp1 Rn00681031_m1						○	A marker of BECs	[66]
None							Negative control	N/A

NOTE. For zonation information obtained from Halpern et al,[18] we referred to Supplementary Table 3 in their article. We defined genes with zonation as those with a *P* value (Kruskal–Wallis) $< .01$. Genes with their expression peak in layers 1–3, 4–6, and 7–9 were defined as zone 1, zone 2, and zone 3 markers, respectively.

Mononucleated 4c Hepatocytes Are More Zone 3–Enriched Than Binucleated 4c Hepatocytes

Finally, we investigated whether nuclearity affects the gene expression profiles of 4c hepatocytes. A recent study examined the difference in metabolic capacity between mononucleated and binucleated hepatocytes.[34] In the present study, we asked whether zonation varies between mononucleated and binucleated 4c hepatocytes. Taking advantage of the single-cell–capturing ability of the C1 platform, we annotated 175 4c hepatocytes with mononuclear or binuclear states (Figure 10*A*). PCA mapping of 106 mononucleated and 69 binucleated hepatocytes did not show a clear separation (Figure 10*B*). However, individual comparison of the expression levels of zonation-related genes showed that mononucleated 4c hepatocytes expressed zone 3–enriched (Figure 10*C*, middle) and zone 1–enriched (Figure 5*C*, bottom left) genes at higher and lower levels, respectively, than binucleated hepatocytes, while nonmonotonic genes were mostly expressed evenly (Figure 10*C*, top row). Except for *Tbx3* ($P = 7.9 \times 10^{-5}$), most LPC marker genes were not expressed differentially between mononucleated and binucleated 4c hepatocytes (Figure 10*C*, bottom right). *Tbx3* is a downstream gene in the Wnt signaling pathway similar to *Axin2*, and therefore its expression supports the idea that mononucleated 4c hepatocytes are enriched in zone 3.[35] Despite this finding, the zonal signature is much more clearly distinguishable between 2c and 4c hepatocytes (Figure 11).

Discussion

This study provides new insights into hepatocyte heterogeneity, namely 2c hepatocytes are preferentially localized to the pericentral region; and a subpopulation of 2c hepatocytes show LPC-like features in terms of LPC marker expression (*Axin2*, *Prom1*, and *Lgr5*).

In a previous study, Lu et al[36] reported no major differences in the gene expression patterns between mouse hepatocytes of different ploidy. Inconsistencies between their observations and ours might derive from differences in, first, the analyzed probe numbers: approximately 12,000 probes (designed based on the information available in 2002) were included in the Lu et al[36] study, whereas approximately 45,000 probes were used in our study; and, second, the microarray platforms: Lu et al[36] used the Affymetrix (Santa Clara, CA) platform, whereas we used the Agilent platform. However, we confirmed that the differentially expressed genes reported by Lu et al[36] also were expressed differentially in our study. Eleven of the 75 probes that correspond to the 56 genes identified as being expressed differentially by Lu et al[36] also were identified as expressed differentially in the present study ($P < .05$, RM 1-way ANOVA). The P values for these 75 probes were significantly lower than those of the whole 35,852 probes ($P = 1.2 \times 10^{-4}$ by the Wilcoxon test) (Figure 12), confirming, at least partly, consistency between the observations of Lu et al[36] and those described here. In addition, we confirmed the enrichment of cell cycle–related genes in 8c hepatocytes, which is consistent with the established notion that polyploidy is formed via cell division failure. Thus, we believe that our analysis successfully identified characteristic features of hepatocytes with different ploidy statuses.

Zonal localization of hepatocytes with different ploidy statuses is an unresolved issue in the field. Our bulk transcriptome and scPCR analysis consistently showed that 2c hepatocytes are localized preferentially to the pericentral region. Specifically, scPCR showed that the hepatocytes with the highest expression levels of *Glul*, one of the most stringent pericentral marker genes, were almost exclusively 2c. The proposition of Wang et al[6] that pericentral hepatocytes are enriched among 2c hepatocytes is consistent with ours. However, their finding does not necessarily indicate that 2c hepatocytes are located in the pericentral region, whereas the present study directly showed that 2c hepatocytes are localized preferentially to the pericentral region. At the same time, the finding that 2c hepatocytes show zone 3–enriched features was surprising because it is widely accepted that diploid hepatocytes are enriched in the periportal region and polyploid hepatocytes are enriched in the pericentral region.[5,10–13] At present, we cannot resolve this discrepancy, but one possible explanation is the methodology-dependent bias of isolated hepatocytes. In the present study, to avoid contamination with BECs, we used a stringent hepatocyte enrichment protocol in which digested whole-liver cells were subjected to sequential centrifugation steps (57 × g for 1 min, 2 cycles) and then separated further using Percoll density gradient centrifugation (see the Materials and Methods section). Our method highly enriches mature hepatocytes but, in turn, possibly loses a minor fraction of smaller hepatocytes, the so-called "small hepatocytes," which are found in both parenchymal and nonparenchymal fractions.[37] Indeed, in this study, the 2c fraction accounted for approximately 5.4% ± 2.2% (means ± SD, n = 16 rats aged between 5 and 14 weeks) of total hepatocytes. This is lower than the widely accepted percentage of 2c hepatocytes: it generally is accepted that approximately 10%–15% of hepatocytes are diploid in rats and mice.[3,5] We cannot rule out the possibility that, in our experiments, some of the 2c hepatocytes were lost. Nonetheless, it still is noteworthy that a substantial number of 2c hepatocytes showed zone 3–enriched characteristics. Moreover, unlike previous studies in which conclusions were drawn based on histologic analyses, this study provides novel insights from the transcriptomic perspective.

This study also provides novel insights into LPC biology. It remains controversial whether the liver has resident stem/progenitor cells. Our scPCR study does not provide direct evidence for their existence but shows instead that 2c hepatocytes are more enriched in well-established LPC markers than 4c hepatocytes. In particular, our data suggest that these progenitor-like cells have a hierarchy in which *Lgr5*$^{+}$*Prom1*$^{+}$*Axin2*$^{+}$ TP cells reside at the top (at least according to the gene set used here). On the other hand, because the sample size in this study was small, in particular for the TP population (11 of 92 and 3 of 245 cells for 2c and 4c populations, respectively), we have to be careful about the conclusion. In addition, our single-cell analysis was based on a limited panel of genes, thereby leaving the

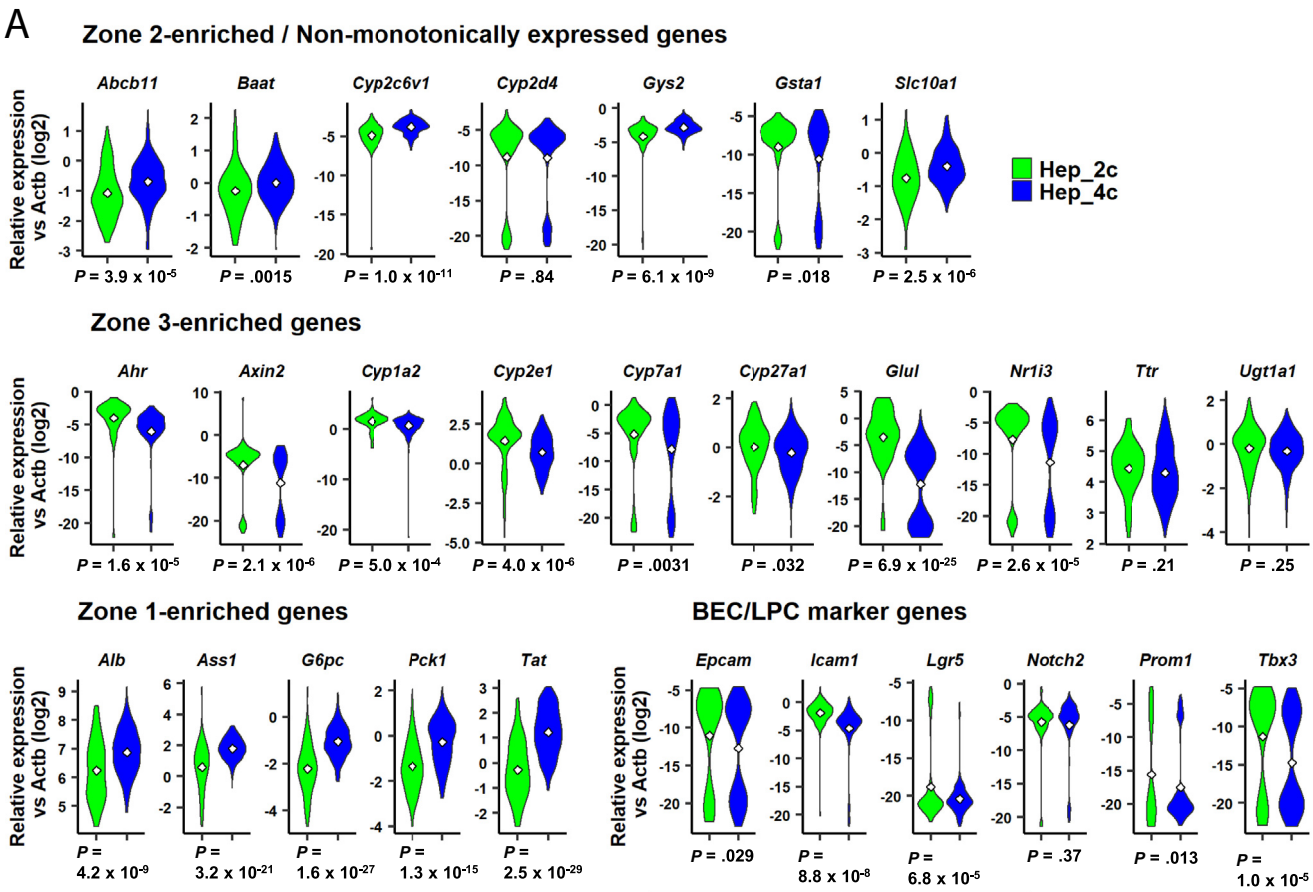
A
Zone 2-enriched / Non-monotonically expressed genes
Abcb11
Baat
Cyp2c6v1
Cyp2d4
Gys2
Gsta1
Slc10a1
Relative expression vs Actb (log2)
Hep_2c
Hep_4c
P = 3.9 x 10-5
P = .0015
P = 1.0 x 10-11
P = .84
P = 6.1 x 10-9
P = .018
P = 2.5 x 10-6
Zone 3-enriched genes
Ahr
Axin2
Cyp1a2
Cyp2e1
Cyp7a1
Cyp27a1
Glul
Nr1i3
Ttr
Ugt1a1
P = 1.6 x 10-5
P = 2.1 x 10-6
P = 5.0 x 10-4
P = 4.0 x 10-6
P = .0031
P = .032
P = 6.9 x 10-25
P = 2.6 x 10-5
P = .21
P = .25
Zone 1-enriched genes
Alb
Ass1
G6pc
Pck1
Tat
P = 4.2 x 10-9
P = 3.2 x 10-21
P = 1.6 x 10-27
P = 1.3 x 10-15
P = 2.5 x 10-29
BEC/LPC marker genes
Epcam
Icam1
Lgr5
Notch2
Prom1
Tbx3
P = .029
P = 8.8 x 10-8
P = 6.8 x 10-5
P = .37
P = .013
P = 1.0 x 10-5
B
Color Key
Row Z-Score
Cell_type
2c_Hep
4c_Hep
Cell_Cluster
Cell_type
Alb
Ttr
Abcc2
Sult2a1
Hnf4a
Tat
Ass1
Cyp2e1
Cyp3a23/3a1
Cyp1a2
Pck1
Cyp27a1
Ugt1a1
Baat
Slc10a1
Abcb11
Cyp2b3
Gapdh
G6pc
Nr1i2
Prom1
Lgr5
Sox9
Cyp2f4
Ahr
Notch2
Icam1
Gys2
Cyp2c6v1
Aldh1a1
Itga6
Hnf1b
Cyp2d4
Gsta1
Epcam
Tbx3
Cyp7a1
Glul
Axin2
Nr1i3

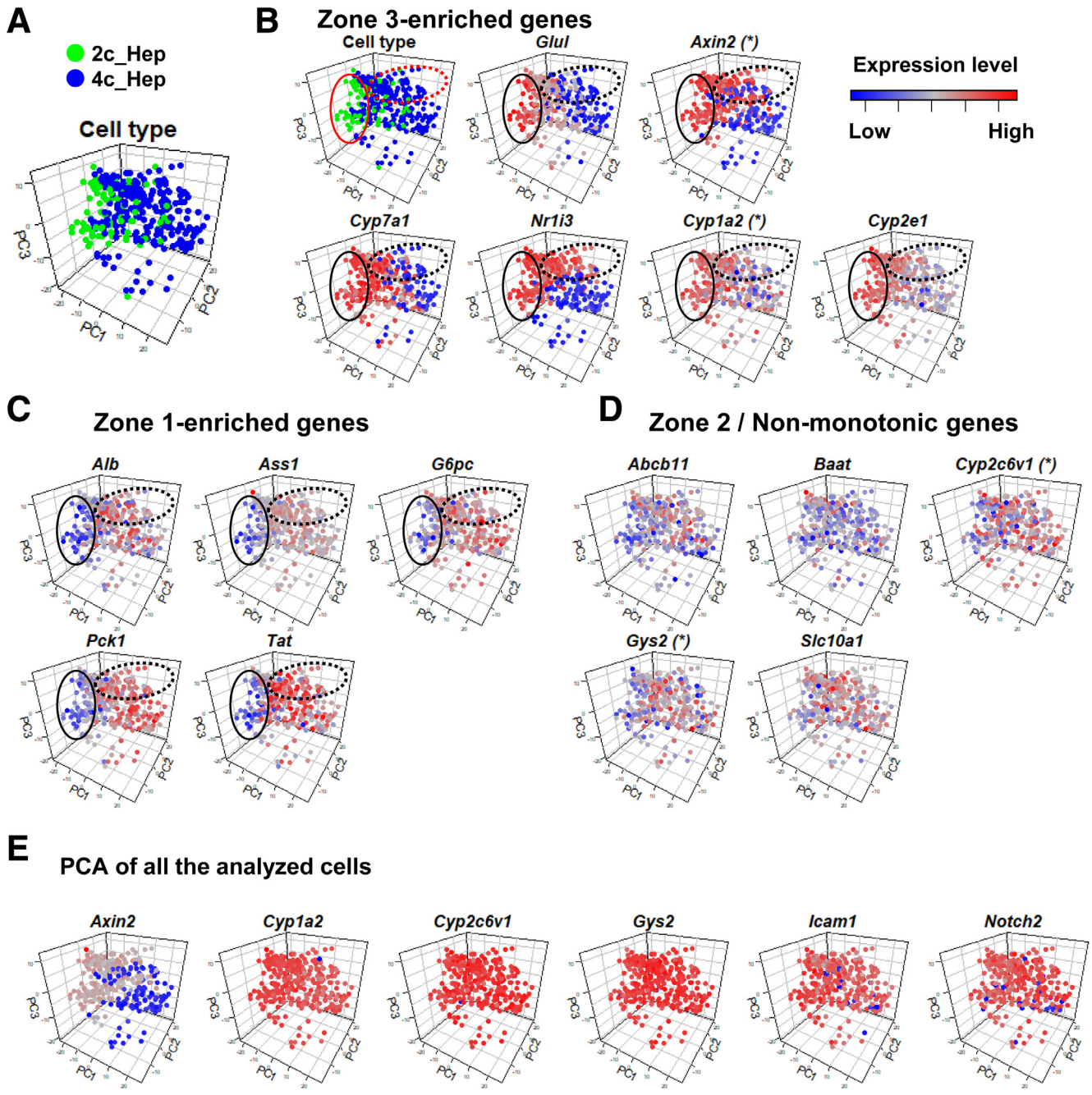

Figure 8. Characterization of 2c and 4c hepatocytes by PCA mapping. (*A*) PCA mapping of 92 2c (green) and 245 4c (blue) hepatocytes. (*B–D*) Each cell is colored according to the designated gene expression level as scaled with the color key. (*B*) *Solid ellipses* and *dotted ellipses* indicate a *Glul*-high 2c cell-rich population and zone 3–oriented 4c cell-rich population, respectively. In panels with *asterisks*, some cells were excluded from the analysis because their inclusion reduced the resolution of the expression profiles for the designated genes. Complete mapping of these genes is shown in panel *E*. (*E*) Complete PCA mapping of 337 hepatocytes for *Axin2*, *Cyp1a2*, *Cyp2c6v1*, *Gys2*, *Icam1*, and *Notch2*.

Figure 7. (***See previous page***). **scPCR-based expression profile of hepatocyte and LPC markers in 2c and 4c hepatocytes.** (*A*) Violin plots of nonmonotonically expressed hepatic genes (*top*), zone 3–enriched genes (*middle*), zone 1–enriched genes (*bottom left*), and LPC marker genes (*bottom right*). Expression level for each gene was normalized with that of *Actb*. *White diamonds* indicate mean values. *P* values were calculated using the Welch *t* test (n = 92 and 245 for 2c and 4c hepatocytes, respectively). (*B*) Heatmap with hierarchical clustering of 92 2c and 245 4c hepatocytes using 40 genes. The *upper* and *lower* column side color bars, designated as "Cell_Cluster" and "Cell_type", indicate 12 cell clusters and hepatocyte ploidy, respectively.

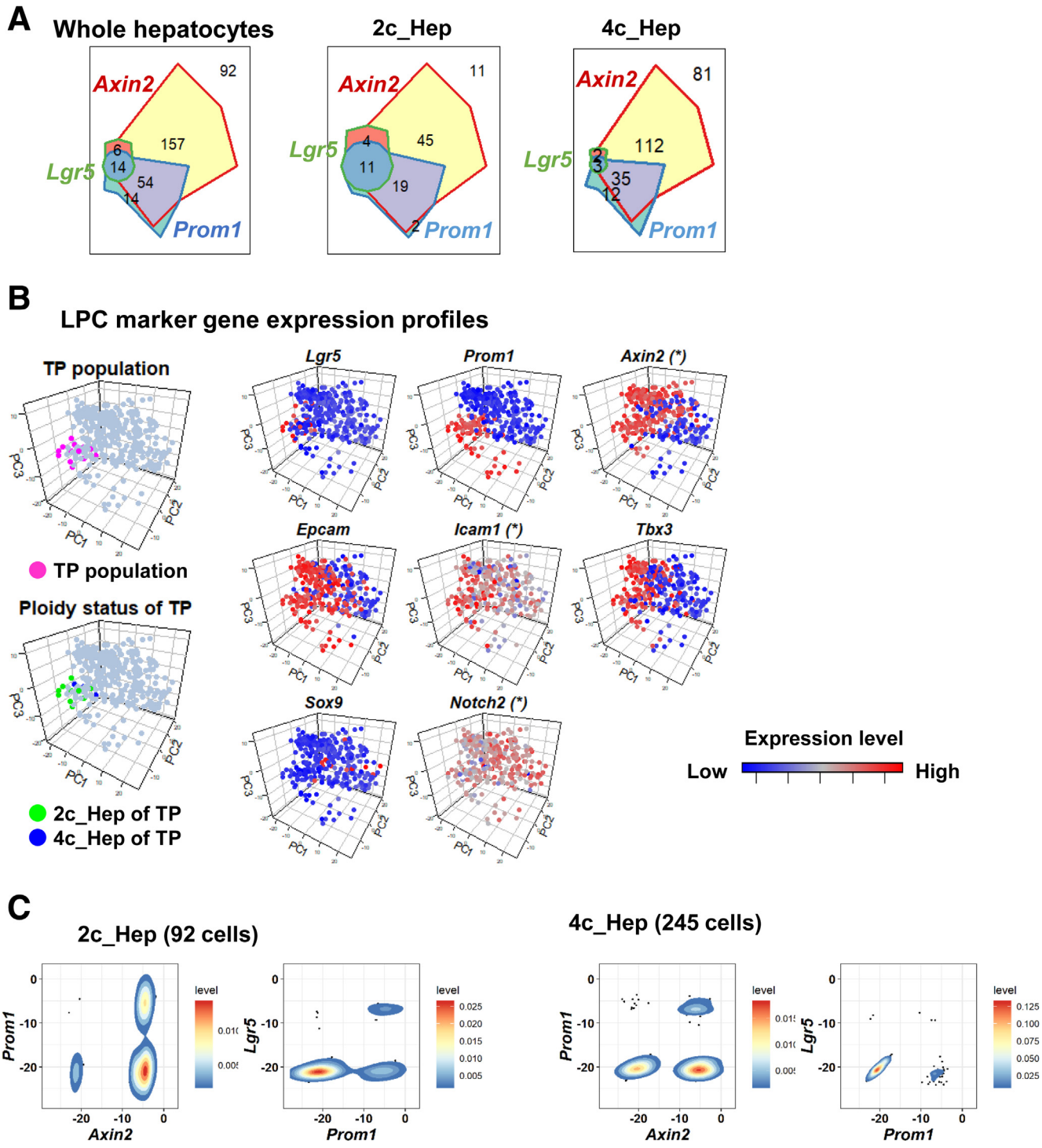

Figure 9. Characterization of LPC-like subpopulation in 2c hepatocytes. (*A*) Venn diagram describing the co-expression profile of 3 LPC marker genes: *Axin2*, *Prom1*, and *Lgr5*. (*B*) Cells of *Axin2*$^{+}$*Prom1*$^{+}$*Lgr5*$^{+}$ TP population are highlighted in magenta (*upper left*). The ploidy status of TP population cells is indicated in green (2c) and blue (4c) (*lower left*). Expression levels for all of the analyzed LPC marker genes are shown (*right*). In panels with *asterisks*, some cells were excluded from the analysis because their inclusion reduced the resolution of the expression profiles for the designated genes. Complete mapping of these genes is shown in Figure 8*E*. (*C*) Scatter plot with density estimations for *Axin2* vs *Prom1* and *Prom1* vs *Lgr5*. Expression levels for each gene are normalized to *Actb*. (*D*) Scatter plot with density estimations for *Axin2* vs *Prom1* and *Prom1* vs *Lgr5*. Expression levels for each gene are normalized to *Actb*.

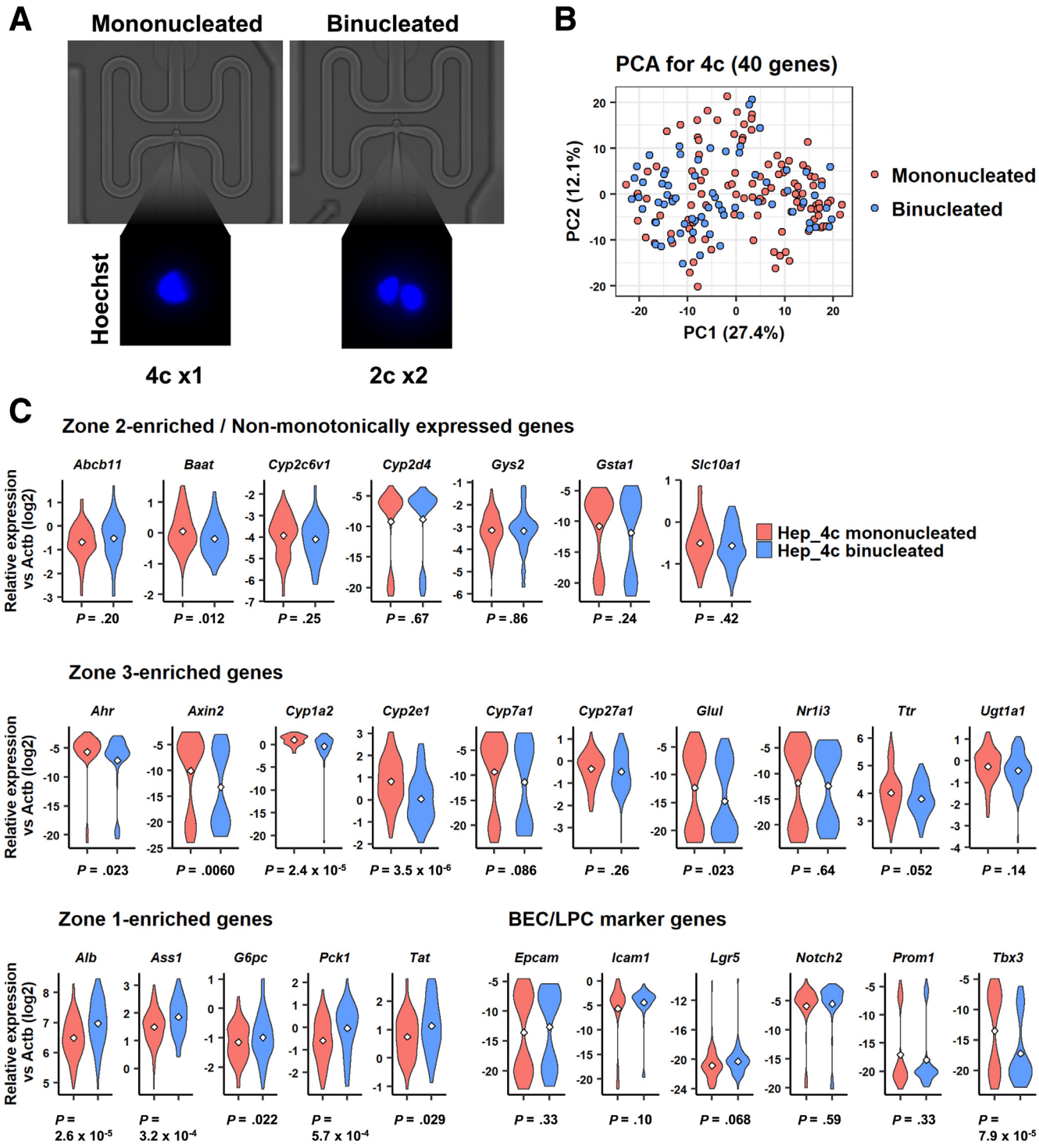

Figure 10. Nuclearity-based dissection of 4c hepatocytes. (*A*) Microscopic identification of the nuclearity of 4c hepatocytes using the C1 microfluidics platform. A total of 106 mononucleated and 69 binucleated hepatocytes were included in this analysis. Images were taken using the BZX-710 microscope (Keyence). (*B*) PCA for mononucleated and binucleated 4c hepatocytes using 40 genes. (*C*) Violin plots of nonmonotonically expressed hepatic genes (*top*), zone 3–enriched genes (*middle*), zone 1–enriched genes (*bottom left*), and LPC marker genes (*bottom right*). *P* values were calculated using the Welch *t* test.

possibility that we have missed other LPC markers that would further dissect the hepatocyte population. Further exploration will require single-cell RNA sequencing with a larger sample scale. Nonetheless, we propose that this study provides a wealth of transcriptomic data and provides some novel insights about localization and function of the heterogeneous population of hepatocytes, which can be tested in the future.

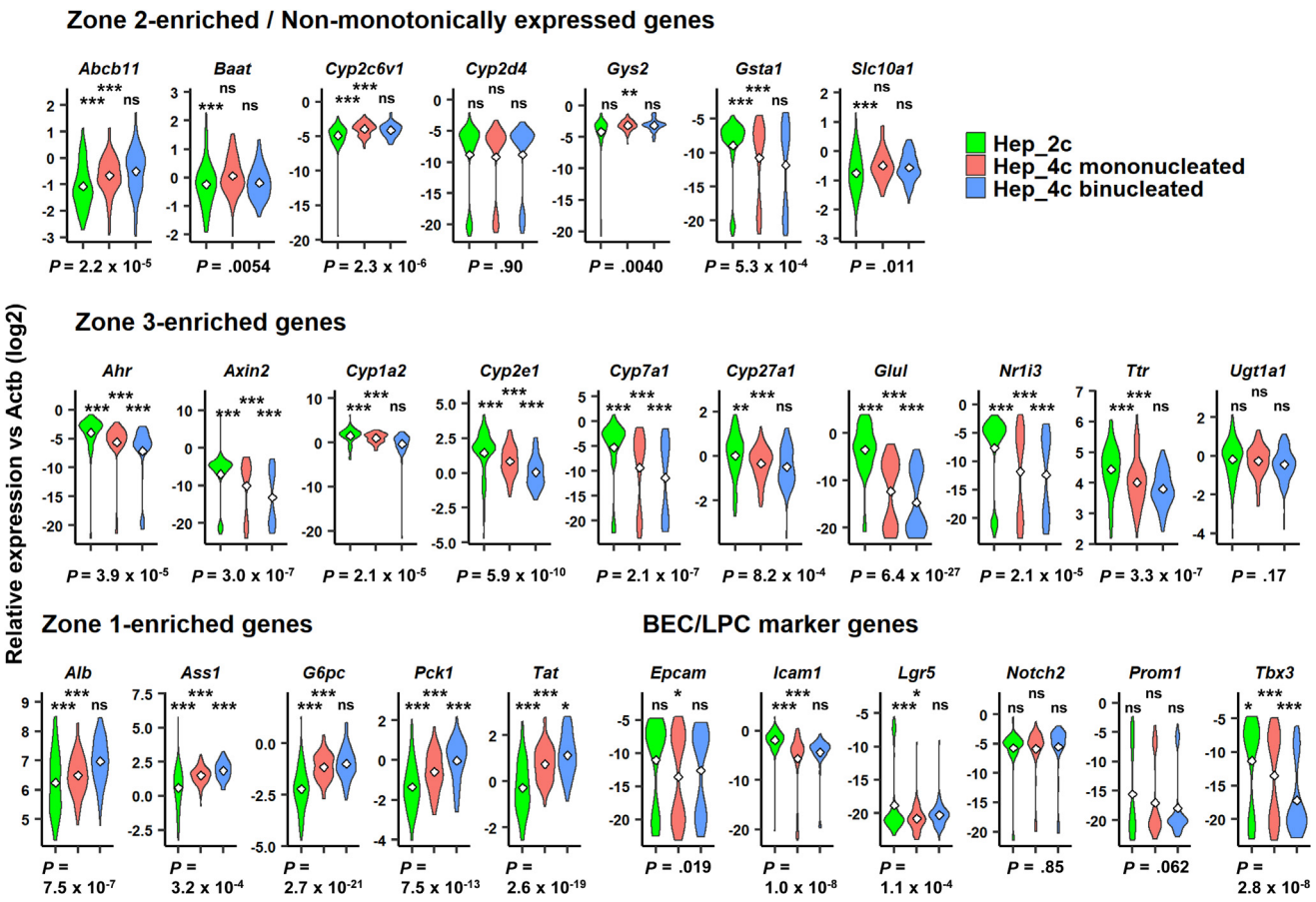

Figure 11. Comparison between mononucleated and binucleated 4c hepatocytes and 2c hepatocytes. Violin plots of nonmonotonically expressed hepatic genes (*top*), zone 3–enriched genes (*middle*), zone 1–enriched genes (*bottom left*), and LPC marker genes (*bottom right*). A total of 92 2c hepatocytes, 106 mononucleated 4c hepatocytes, and 69 binucleated 4c hepatocytes were used. *P* values at the bottom of each panel were calculated by 1-way ANOVA, followed by the Tukey multiple comparisons test. *P* values for post hoc tests are presented as follows: $^{*}P < .05$, $^{**}P < .01$, $^{***}P < .001$. Significance symbols on the *left*, *middle*, and *right* in each panel indicate the comparison between 2c and mononucleated 4c hepatocytes, 2c and binonucleated 4c hepatocytes, and mononucleated and binucleated 4c hepatocytes, respectively.

Finally, we clarify the limitation of the present study. First, given the interspecies difference in ploidy profile of hepatocytes, the relevance of our findings here is not applicable simply to human liver biology. The degree of liver polyploidization varies between mammals: although 80%–97%[9,34,38–40] and 70%–95%[41–44] of adult mouse and rat hepatocytes are polyploid, respectively, only 10%–40% of adult human hepatocytes are polyploid.[45–47] Strikingly, although polyploid hepatocytes become the majority within a week after weaning in rodents, polyploid cells generally do not exceed 15% in 20-year-old human beings. These reports collectively suggest that the role division that might be provided by the ploidy heterogeneity is different between rodents and human beings. Further study with the use of freshly isolated human hepatocytes will be required.

Materials and Methods

Rats

Animal experiments in this study were performed in compliance with the guidelines of the Institute for Laboratory Animal Research of the National Cancer Center Research Institute. The protocol was approved by the Committee on the Ethics of Animal Experiments of the National Cancer Center Research Institute. Rats were housed in specific pathogen-free facilities on a 12-hour light/dark cycle and were given food and water ad libitum. All animals used in this study were female Wistar rats aged between 5 and 14 weeks (CLEA Japan, Shizuoka, Japan). Details regarding the animals used in the study are described for each part of the experiment in the Materials and Methods section.

Isolation of Rat Adult Hepatocytes

Adult rat hepatocytes were isolated from using the procedure described by Seglen[48] with minor modifications (for details, see Katsuda et al[49]). Briefly, after preperfusion with Ca^{2+}-free Hank's/ethylene glycol-bis(β-aminoethyl ether)-*N,N,N′,N′*-tetraacetic acid solution through the portal vein, the liver was perfused with approximately 400 mL Hank's solution containing 0.05% collagenase at 25–30 mL/

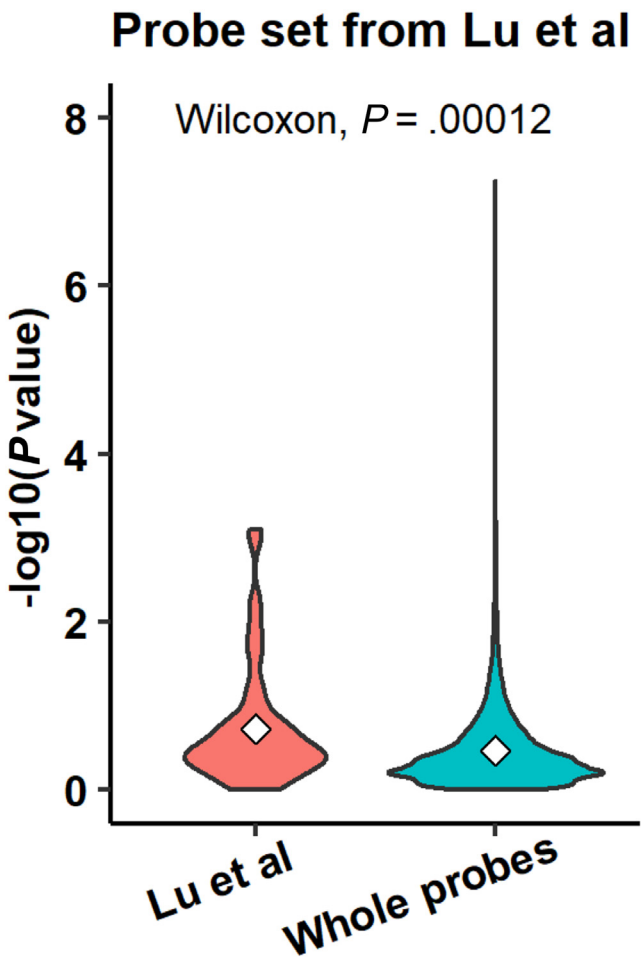

Figure 12. Analysis of genes that were reported to be expressed differentially among hepatocytes with different ploidy status. *P* values were calculated by RM 1-way ANOVA using 2c, 4c, and 8c hepatocytes (n = 5 experiments) for 75 probes, which correspond to the 56 differentially expressed genes reported by Lu et al[36] and compared with the *P* values for whole probes (n = 75 probes for Lu et al[36]; n = 18,021 probes for whole probes).

min. The extracted liver was mechanically digested with a surgical knife and then enzymatically digested in a mixture of 0.05% collagenase solution and 20 mL E-MEM (Sigma, St. Louis, MO) at 37°C for 15 minutes. The digested liver then was filtered twice through a sterilized cotton mesh (single-folded and then double-folded). The cell suspension was aliquoted into two 50-mL tubes, which then were filled with E-MEM, and the cells were collected via centrifugation at 57 × *g* for 1 minute. After resuspension in a 50 mL/tube E-MEM, large-cell aggregates were eliminated by filtering the cell suspension through a 60-μm stainless double-mesh cell strainer (Ikemoto Scientific Technology Co, Ltd, Tokyo, Japan) and the cells were collected by centrifuging the filtrate at 57 × *g* for 1 minute. Next, the cells were resuspended in 24.5 mL/tube complete Percoll medium (25 mL L-15 medium [Life Technologies, Carlsbad, CA] supplemented with 0.429 g/L HEPES [Sigma], 2 g/L bovine serum albumin [Sigma], 1 × 10^{-7} mol/L insulin [Sigma], 2.4 mL 10× Hank's balanced salt solution(-) [Life Technologies], and 21.6 mL Percoll [GE Healthcare, Chicago, IL]), and dead cells were removed via centrifugation at 57 × *g* for 10 minutes. Finally, the cells were washed in 50 mL/tube E-MEM twice via centrifugation at 57 × *g* for 2 minutes. The purified hepatocytes were used for the downstream experiments.

Isolation of BEC-Enriched NPCs

NPCs were isolated from 7-week-old rats as described previously.[50,51] Briefly, we harvested bile duct containing remnant tissue after 2-step collagenase perfusion of an adult rat liver as described earlier. Then, the remnant tissue was digested by shaking at 37°C for 30 minutes in Leibovitz L-15 medium (Invitrogen, Carlsbad, CA) supplemented with 400 U/mL collagenase (Wako, Tokyo, Japan), 700 U/mL hyaluronidase (Sigma-Aldrich), 10^{-7} mol/L insulin, and 10^{-7} mol/L dexamethasone. After filtration with a 40-mm cell strainer (BD Biosciences, Franklin Lakes, NJ), the cells were collected by centrifugation at 800 × *g* for 10 minutes. Then the pellet was resuspended in Dulbecco's modified Eagle medium (Invitrogen) supplemented with 10% fetal bovine serum (Invitrogen) and centrifuged twice at 800 × *g* for 5 minutes. Purified NPCs were captured by the C1 Auto Prep system and analyzed by scPCR.

FACS of Hepatocytes With Different Ploidy Statuses

To fractionate the 2c, 4c, and 8c hepatocytes, FACS-based single-cell isolation was performed according to a previously described protocol.[39] Briefly, rat hepatocytes harvested from 5- to 14-week old rats were suspended in 10% fetal bovine serum–Dulbecco's modified Eagle medium supplemented with 15 mg/mL Hoechst 33342 and 5 μmol/L reserpine and incubated at 37°C for 10 minutes. After the addition of 5 μg/mL propidium iodide (BD Biosciences), the cells were sorted using a FACSAria II or FACSAria III (BD Biosciences).

Colony Formation Assay of Single 2c, 4c, and 8c Rat Hepatocytes

Hepatocytes harvested from 5- to 8-week-old rats were sorted into 96-well collagen-coated plates filled with 100 μL/well of Dulbecco's modified Eagle medium/F12 (Life Technologies) containing 2.4 g/L $NaHCO_3$ and L-glutamine, which was supplemented with 5 mmol/L HEPES (Sigma), 30 mg/L L-proline (Sigma), 0.05% bovine serum albumin (Sigma), 10 ng/mL epidermal growth factor (Sigma), insulin-transferrin-serine-X (Life Technologies), 10^{-7} mol/L dexamethasone (Sigma), 10 mmol/L nicotinamide (Sigma), 1 mmol/L ascorbic acid-2 phosphate (Wako), an antibiotic/antimycotic solution (Life Technologies), and 3 small molecules: 10 µmol/L Y-27632 (Wako), 0.5 µmol/L A-83-01 (Wako), and 3 µmol/L CHIR99021 (Axon Medchem, Reston, VA). On day 1, the cell and nuclei number for each well was determined, and wells that contained dead cells and, in the 8c plates, cells greater than doublets were excluded from

further analysis. Ten days after seeding, cells from each of the formed colonies were counted manually.

Microarray Analysis

Hepatocytes isolated from 5 rats aged between 5 and 14 weeks were used. A 1-color microarray-based gene expression analysis system (Agilent Technologies, Santa Clara, CA) using the SurePrint G3 Rat GE 8 × 60 K Kit (G4853A) was used following the manufacturer's instructions. Normalization was performed using Agilent GeneSpring version 12.6.1 (per chip: normalization to 75th percentile shift; per gene: normalization to the median of all samples). Probes with signal values lower than 5 in average (75 of total signal value for the 15 samples) were excluded from further analysis. The intensity values were $\log_2$-transformed, and RM 1-way ANOVA was performed using the lmne R package to identify differentially expressed genes. Probes with *P* values less than .05 were regarded as differentially expressed. Unsupervised clustering was performed using the heatmap.2 or heatmap.3 R package. PCA was performed using the prcomp R package, and mapped with the ggplot2 R package. Pathway analysis was performed using the clusterProfiler R package.[52]

Measurement of Cell Diameter of 2c, 4c, and 8c Hepatocytes

FACS-sorted hepatocytes isolated from a 9-week-old rat were sparsely loaded into a hemocytometer and imaged with a Keyence BZX-710 camera (Keyence, Osaka, Japan). Cell area was calculated using the Hybrid Cell Count program (Keyence). Cell diameter was determined using the following equation: $2\sqrt{(area/\pi)}$.

Capturing Single Cells

Single-cell capture, lysis, and RT pre-amplification experiments were performed using the C1 Auto Prep System (Fluidigm, South San Francisco, CA) according to the manufacturer's instructions. Isolated hepatocytes and NPCs were loaded into the C1 integrated fluidic circuit at a concentration of 300 cells/μL in phosphate-buffered saline containing 5% fetal bovine serum and 5 mmol/L of EDTA (Nacalai Tesque, San Diego, CA). Once cell capture was archived, cells were assessed for viability stain using Calcein-AM and ethidium homodimer 1 (Live/Dead Kit; Life Technologies). Chips were imaged using a BZ-X710 and chambers containing 2 or more, none, or dead cells were removed from further analysis. After lysis, reverse transcription (25°C for 10 min, 42°C for 60 min, 85°C for 5 min) and pre-amplification for 18 cycles (each cycle: 95°C for 15 sec, 60°C for 4 min), single-cell complementary DNA was harvested, transferred to a 96-well plate, and diluted 6 times with complementary DNA dilution buffer.

Single-Cell scPCR

For this study, hepatocytes isolated from 5- to 7-week-old rats were used. Single-cell gene-expression experiments were performed using Fluidigm's 96.96 or 48.48 quantitative PCR DynamicArray microfluidic chips (Fluidigm) according to the manufacturer's instructions. Individual probe assay mixes were generated by loading 2.5 μL of 2× Assay Loading Reagent (Fluidigm) and 2.5 μL 20× TaqMan gene expression assay (Applied Biosystems, Beverly, MA). Sample mixes were generated by 2.5 μL 2× TaqMan Universal PCR Master Mix (Applied Biosystems), 0.25 μL of 20× GE Sample Loading Reagent (Fluidigm), and 2.25 μL of diluted complementary DNA. Plates were vortexed and centrifuged to homogenize the solutions. Before loading probe assays and sample mixes into 96.96 or 48.48 DynamicArray microfluidic chips, chips were primed in a HX integrated fluidic circuit controller (Fluidigm) machine. After priming, 5 μL of both sample and probe mix were loaded individually in the same machine. Then, chips were transferred into the BioMarkHD real-time quantitative PCR (Fluidigm) and run according to the manufacturer's instructions. Expression levels were normalized with *Actb*.

Statistics

When comparing 2 means, *P* values were calculated by the Welch *t* test unless otherwise mentioned. Paired comparisons for more than 2 means was conducted using RM 1-way ANOVA, followed by the Holm multiple comparisons test. Unpaired comparisons for more than 2 means were conducted using 1-way ANOVA, followed by the Tukey multiple comparisons test.

Accession Numbers

The microarray data are deposited in GEO under accession number GSE132409. The raw data of scPCR (cycle threshold values) are deposited in GEO under accession number GSE132459.

References

1. Gentric G, Celton-Morizur S, Desdouets C. Polyploidy and liver proliferation. Clin Res Hepatol Gastroenterol 2012;36:29–34.
2. Wang MJ, Chen F, Lau JTY, Hu YP. Hepatocyte polyploidization and its association with pathophysiological processes. Cell Death Dis 2017;8:e2805.
3. Gentric G, Desdouets C. Polyploidization in liver tissue. Am J Pathol 2014;184:322–331.
4. Pandit SK, Westendorp B, De Bruin A. Physiological significance of polyploidization in mammalian cells. Trends Cell Biol 2013;23:556–566.
5. Duncan AW. Aneuploidy, polyploidy and ploidy reversal in the liver. Semin Cell Dev Biol 2013;24:347–356.
6. Wang B, Zhao L, Fish M, Logan CY, Nusse R. Self-renewing diploid Axin2+ cells fuel homeostatic renewal of the liver. Nature 2015;524:180–185.
7. Katsuda T, Kawamata M, Hagiwara K, Takahashi RU, Yamamoto Y, Camargo FD, Ochiya T. Conversion of terminally committed hepatocytes to culturable bipotent progenitor cells with regenerative capacity. Cell Stem Cell 2017;20:41–55.

8. Wilkinson PD, Delgado ER, Alencastro F, Leek MP, Roy N, Weirich MP, Stahl EC, Otero PA, Chen MI, Brown WK, Duncan AW. The polyploid state restricts hepatocyte proliferation and liver regeneration. Hepatology 2019;69:1242–1258.
9. Zhang S, Zhou K, Luo X, Li L, Tu HC, Sehgal A, Nguyen LH, Zhang Y, Gopal P, Tarlow BD, Siegwart DJ, Zhu H. The polyploid state plays a tumor-suppressive role in the liver. Dev Cell 2018;44:447–459.e5.
10. Tanami S, Ben-Moshe S, Elkayam A, Mayo A, Bahar Halpern K, Itzkovitz S. Dynamic zonation of liver polyploidy. Cell Tissue Res 2017;368:405–410.
11. Schmucker DL. Hepatocyte fine structure during maturation and senescence. J Electron Microsc Tech 1990; 14:106–125.
12. Chao HW, Doi M, Fustin JM, Chen H, Murase K, Maeda Y, Hayashi H, Tanaka R, Sugawa M, Mizukuchi N, Yamaguchi Y, Yasunaga JI, Matsuoka M, Sakai M, Matsumoto M, Hamada S, Okamura H. Circadian clock regulates hepatic polyploidy by modulating Mkp1-Erk1/2 signaling pathway. Nat Commun 2017;8:1–14.
13. Asahina K, Shiokawa M, Ueki T, Yamasaki C, Aratani A, Tateno C, Yoshizato K. Multiplicative mononuclear small hepatocytes in adult rat liver: their isolation as a homogeneous population and localization to periportal zone. Biochem Biophys Res Commun 2006;342:1160–1167.
14. Gebhardt R, Matz-Soja M. Liver zonation: novel aspects of its regulation and its impact on homeostasis. World J Gastroenterol 2014;20:8491–8504.
15. Torre C, Perret C, Colnot S. Molecular determinants of liver zonation. Prog Mol Biol Transl Sci 2010;97:127–150.
16. Oinonen T, Lindros KO. Zonation of hepatic cytochrome P-450 expression and regulation. Biochem J 1998; 329:17–35.
17. Jungermann K, Keitzmann T. Zonation of parenchymal and nonparenchymal metabolism in liver. Annu Rev Nutr 1996;16:179–203.
18. Halpern KB, Shenhav R, Matcovitch-Natan O, Tóth B, Lemze D, Golan M, Massasa EE, Baydatch S, Landen S, Moor AE, Brandis A, Giladi A, Stokar-Avihail A, David E, Amit I, Itzkovitz S. Single-cell spatial reconstruction reveals global division of labour in the mammalian liver. Nature 2017;542:352–356.
19. Behari J. The Wnt/β-catenin signaling pathway in liver biology and disease. Expert Rev Gastroenterol Hepatol 2010;4:745–756.
20. Russell JO, Monga SP. Wnt/β-catenin signaling in liver development, homeostasis, and pathobiology. Annu Rev Pathol 2018;13:351–378.
21. Miyajima A, Tanaka M, Itoh T. Stem/progenitor cells in liver development, homeostasis, regeneration, and reprogramming. Cell Stem Cell 2014;14:561–574.
22. Lin S, Nascimento EM, Gajera CR, Chen L, Neuhöfer P, Garbuzov A, Wang S, Artandi SE. Distributed hepatocytes expressing telomerase repopulate the liver in homeostasis and injury. Nature 2018;556:244–248.
23. Font-Burgada J, Shalapour S, Ramaswamy S, Hsueh B, Rossell D, Umemura A, Taniguchi K, Nakagawa H, Valasek MA, Ye L, Kopp JL, Sander M, Carter H, Deisseroth K, Verma IM, Karin M. Hybrid periportal hepatocytes regenerate the injured liver without giving rise to cancer. Cell 2015;162:766–779.
24. Tanimizu N, Ichinohe N, Yamamoto M, Akiyama H, Nishikawa Y, Mitaka T. Progressive induction of hepatocyte progenitor cells in chronically injured liver. Sci Rep 2017;7:39990.
25. Yimlamai D, Christodoulou C, Galli GG, Yanger K, Pepe-Mooney B, Gurung B, Shrestha K, Cahan P, Stanger BZ, Camargo FD. Hippo pathway activity influences liver cell fate. Cell 2014;157:1324–1338.
26. Yanger K, Zong Y, Maggs LR, Shapira SN, Maddipati R, Aiello NM, Thung SN, Wells RG, Greenbaum LE, Stanger BZ. Robust cellular reprogramming occurs spontaneously during liver regeneration. Genes Dev 2013;27:719–724.
27. Tarlow BDD, Pelz C, Naugler WEE, Wakefield L, Wilson EM, Finegold MJ, Grompe M. Bipotential adult liver progenitors are derived from chronically injured mature hepatocytes. Cell Stem Cell 2014;15:605–618.
28. Tanimizu N, Nishikawa Y, Ichinohe N, Akiyama H, Mitaka T. Sry HMG box protein 9-positive (Sox9+) epithelial cell adhesion molecule-negative (EpCAM-) biphenotypic cells derived from hepatocytes are involved in mouse liver regeneration. J Biol Chem 2014; 289:7589–7598.
29. Yovchev MI, Locker J, Oertel M. Biliary fibrosis drives liver repopulation and phenotype transition of transplanted hepatocytes. J Hepatol 2016;64:1348–1357.
30. Schaub JR, Huppert KA, Kurial SNT, Hsu BY, Cast AE, Donnelly B, Karns RA, Chen F, Rezvani M, Luu HY, Mattis AN, Rougemont AL, Rosenthal P, Huppert SS, Willenbring H. De novo formation of the biliary system by TGFβ-mediated hepatocyte transdifferentiation. Nature 2018;557:247–251.
31. Huch M, Dorrell C, Boj SF, van Es JH, Li VS, van de Wetering M, Sato T, Hamer K, Sasaki N, Finegold MJ, Haft A, Vries RG, Grompe M, Clevers H. In vitro expansion of single Lgr5+ liver stem cells induced by Wnt-driven regeneration. Nature 2013;494:247–250.
32. Han X, Wang Y, Pu W, Huang X, Qiu L, Li Y, Yu W, Zhao H, Liu X, He L, Zhang L, Ji Y, Lu J, Lui KO, Zhou B. Lineage tracing reveals the bipotency of SOX9+ hepatocytes during liver regeneration. Stem Cell Reports 2019;12:624–638.
33. Planas-Paz L, Orsini V, Boulter L, Calabrese D, Pikiolek M, Nigsch F, Xie Y, Roma G, Donovan A, Marti P, Beckmann N, Dill MT, Carbone W, Bergling S, Isken A, Mueller M, Kinzel B, Yang Y, Mao X, Nicholson TB, Zamponi R, Capodieci P, Valdez R, Rivera D, Loew A, Ukomadu C, Terracciano LM, Bouwmeester T, Cong F, Heim MH, Forbes SJ, Ruffner H, Tchorz JS. The RSPO-LGR4/5-ZNRF3/RNF43 module controls liver zonation and size. Nat Cell Biol 2016;18:467–479.
34. Kreutz C, MacNelly S, Follo M, Wäldin A, Binninger-Lacour P, Timmer J, Bartolomé-Rodríguez MM. Hepatocyte ploidy is a diversity factor for liver homeostasis. Front Physiol 2017;8:1–15.
35. Renard CA, Labalette C, Armengol C, Cougot D, Wei Y, Cairo S, Pineau P, Neuveut C, de Reyniès A, Dejean A,

Perret C, Buendia MA. Tbx3 is a downstream target of the Wnt/β-catenin pathway and a critical mediator of β-catenin survival functions in liver cancer. Cancer Res 2007;67:901–910.
36. Lu P, Prost S, Caldwell H, Tugwood JD, Betton GR, Harrison DJ. Microarray analysis of gene expression of mouse hepatocytes of different ploidy. Mamm Genome 2007;18:617–626.
37. Mitaka T. The current status of primary hepatocyte culture. Int J Exp Pathol 1998;79:393–409.
38. Hsu SH, Delgado ER, Otero PA, Teng KY, Kutay H, Meehan KM, Moroney JB, Monga JK, Hand NJ, Friedman JR, Ghoshal K, Duncan AW. MicroRNA-122 regulates polyploidization in the murine liver. Hepatology 2016;64:599–615.
39. Duncan AW, Taylor MH, Hickey RD, Hanlon Newell AE, Lenzi ML, Olson SB, Finegold MJ, Grompe M. The ploidy conveyor of mature hepatocytes as a source of genetic variation. Nature 2010;467:707–710.
40. Wang MJ, Chen F, Li JX, Liu CC, Zhang HB, Xia Y, Yu B, You P, Xiang D, Lu L, Yao H, Borjigin U, Yang GS, Wangensteen KJ, He ZY, Wang X, Hu YP. Reversal of hepatocyte senescence after continuous in vivo cell proliferation. Hepatology 2014;60:349–361.
41. Gandillet A, Alexandre E, Holl V, Royer C, Bischoff P, Cinqualbre J, Wolf P, Jaeck D, Richert L. Hepatocyte ploidy in normal young rat. Comp Biochem Physiol A Mol Integr Physiol 2003;134:665–673.
42. Gorla GR, Malhi H, Gupta S, Gupta S. Polyploidy associated with oxidative injury attenuates proliferative potential of cells. J Cell Sci 2001;114:2943–2951.
43. Lamas E, Chassoux D, Decaux J, Brechot C, Debey P. Quantitative fluorescence imaging approach for the study of polyploidization in hepatocytes. J Histochem Cytochem 2009;51:1–12.
44. Schwarze PE, Pettersen EO, Shoaib MC, Seglen PO. Emergence of a population of small, diploid hepatocytes during hepatocarcinogenesis. Carcinogenesis 1984; 5:1267–1275.
45. Bou-Nader M, Caruso S, Donne R, Celton-Morizur S, Calderaro J, Gentric G, Cadoux M, L'Hermitte A, Klein C, Guilbert T, Albuquerque M, Couchy G, Paradis V, Couty JP, Zucman-Rossi J, Desdouets C. Polyploidy spectrum: a new marker in HCC classification. Gut 2019, Epub ahead of print.
46. Toyoda H, Bregerie O, Vallet A, Nalpas B, Pivert G, Brechot C, Desdouets C. Changes to hepatocyte ploidy and binuclearity profiles during human chronic viral hepatitis. Gut 2005;54:297–302.
47. Kudryavtsev BN, Kudryavtseva MV, Sakuta GA, Stein GI. Human hepatocyte polyploidization kinetics in the course of life cycle. Virchows Arch B Cell Pathol Incl Mol Pathol 1993;64:387–393.
48. Seglen PO. Preparation of isolated rat liver cells. Methods Cell Biol 1976;13:29–83.
49. Katsuda T, Hosaka K, Ochiya T. Generation of chemically induced liver progenitors (CLiPs) from rat adult hepatocytes. Bioprotocol 2018;7:1–26.
50. Katsuda T, Ochiya T, Sakai Y. Generation of hepatic organoids with biliary structures. Methods Mol Biol 2019; 1905:175–185.
51. Katsuda T, Kojima N, Ochiya T, Sakai Y. Biliary epithelial cells play an essential role in the reconstruction of hepatic tissue with a functional bile ductular network. Tissue Eng Part A 2013;19:2402–2411.
52. Yu G, Wang L-G, Han Y, He Q-Y. clusterProfiler: an R package for comparing biological themes among gene clusters. OMICS 2012;16:284–287.
53. Septer S, Edwards G, Gunewardena S, Wolfe A, Li H, Daniel J, Apte U. Yes-associated protein is involved in proliferation and differentiation during postnatal liver development. AJP Gastrointest Liver Physiol 2012; 302:G493–G503.
54. Jungermann K, Kietzmann T. Oxygen: modulator of metabolic zonation and disease of the liver. Hepatology 2000;31:255–260.
55. Braeuning A, Ittrich C, Köhle C, Hailfinger S, Bonin M, Buchmann A, Schwarz M. Differential gene expression in periportal and perivenous mouse hepatocytes. FEBS J 2006;273:5051–5061.
56. Maronpot RR, Yoshizawa K, Nyska A, Harada T, Flake G, Mueller G, Singh B, Ward JM. Liver enlargement–STP regulatory policy papers: hepatic enzyme induction: histopathology. Toxicol Pathol 2010;38:776–795.
57. Antoniou A, Raynaud P, Cordi S, Zong Y, Tronche F, Stanger BZ, Jacquemin P, Pierreux CE, Clotman F, Lemaigre FP. Intrahepatic bile ducts develop according to a new mode of tubulogenesis regulated by the transcription factor SOX9. Gastroenterology 2009; 136:2325–2333.
58. Strazzabosco M, Fabris L. Neural cell adhesion molecule and polysialic acid in ductular reaction: the puzzle is far from completed, but the picture is becoming more clear. Hepatology 2014;60:1469–1472.
59. Schmelzer E, Zhang L, Bruce A, Wauthier E, Ludlow J, Yao HL, Moss N, Melhem A, McClelland R, Turner W, Kulik M, Sherwood S, Tallheden T, Cheng N, Furth ME, Reid LM. Human hepatic stem cells from fetal and postnatal donors. J Exp Med 2007;204:1973–1987.
60. Spee B, Carpino G, Schotanus BA, Katoonizadeh A, Vander Borght S, Gaudio E, Roskams T. Characterisation of the liver progenitor cell niche in liver diseases: potential involvement of Wnt and Notch signalling. Gut 2009;59:247–257.
61. Tanimizu N, Ichinohe N, Ishii M, Kino J, Mizuguchi T, Hirata K, Mitaka T. Liver progenitors isolated from adult healthy mouse liver efficiently differentiate to functional hepatocytes in vitro and repopulate liver tissue. Stem Cells 2016;34:2889–2901.
62. Tanimizu N, Miyajima A. Molecular mechanism of liver development and regeneration. Int Rev Cytol 2007; 259:1–48.
63. Mitaka T, Sato F, Mizuguchi T, Yokono T, Mochizuki Y. Reconstruction of hepatic organoid by rat small hepatocytes and hepatic nonparenchymal cells. Hepatology 1999;29:111–125.
64. Lowes KN, Brennan BA, Yeoh GC, Olynyk JK. Oval cell numbers in human chronic liver diseases are directly related to disease severity. Am J Pathol 1999; 154:537–541.

65. Sell S. Comparison of liver progenitor cells in human atypical ductular reactions with those seen in experimental models of liver injury. Hepatology 1998;27:317–331.
66. Español-Suñer R, Carpentier R, Van Hul N, Legry V, Achouri Y, Cordi S, Jacquemin P, Lemaigre F, Leclercq IA. Liver progenitor cells yield functional hepatocytes in response to chronic liver injury in mice. Gastroenterology 2012;143:1564–1575.e7.

Received March 31, 2019. Accepted August 22, 2019.

Correspondence
Address correspondence to: Takahiro Ochiya, PhD, Institute of Medical Science, Tokyo Medical University, 6-7-1 Nishi-Shinjuku, Shinjuku-ku, Tokyo, 160-0023, Japan. e-mail: tochiya@tokyo-med.ac.jp; fax: (81)-3-6302-0265.

Acknowledgments
The authors thank Ryou-u Takahashi and Hirokazu Ohata for assistance with FACS experiments, Ayako Inoue for technical assistance, and Luc Gailhouste for constructive discussion. The authors also thank Hideki Nishikawa (Keyence Corporation) for assistance with the microscopic analyses.

Takeshi Katsuda is currently at Perelman School of Medicine, University of Pennsylvania, Philadelphia, Pennsylvania 19104.

Author contributions
Takahiro Ochiya supervised the project; Takeshi Katsuda and Kazunori Hosaka designed the experiments; Kazunori Hosaka performed the majority of the experiments with support from Takeshi Katsuda, Juntaro Matsuzaki, Wataru Usuba, Marta Prieto-Vila, and Tomoko Yamaguchi; Takeshi Katsuda analyzed the data with assistance from Kazunori Hosaka; Atsunori Tsuchiya and Shuji Terai assisted with data interpretation and provided helpful discussions; Takeshi Katsuda wrote the manuscript with support from Kazunori Hosaka, Juntaro Matsuzaki, and Takahiro Ochiya; and Takahiro Ochiya and Takeshi Katsuda obtained funding for the study.

Conflicts of interest
The authors disclose no conflicts.

Funding
Supported by Grants-in-Aid from the Research Program on Hepatitis from the Japan Agency for Medical Research and Development (AMED: 16fk0310512h0005 and 17fk0310101h0001 to T.O.) and Japan Society for the Promotion of Science (JSPS) Grant-in-Aid for Young Scientists B (16K16643 to T.K.).